Università degli studi di Torino

SCUOLA DI SCIENZE DELLA NATURA

Corso di Laurea Magistrale in Fisica dei Sistemi Complessi

Tesi di Laurea Magistrale

THE FANCY TITLE OF MY FANCY THESIS

Relatore:
Prof. Michele Caselle

Co-relatore:
Dott. Matteo Osella

Candidato:
Filippo Valle

Controrelatore:
Dott. Matteo Cereda

Anno Accademico 2018/2019

Computers are incredibly fast, accurate, and stupid.
Human beings are incredibly slow, inaccurate, and brilliant.
Together they are powerful beyond imagination Albert Einstein,

Abstract

The interest in studying complex systems is increasingly spreading. Complex systems can be found anywhere and many common behaviours are observable, systems with different origins and purposes may share, for instance, some statistical laws.

An example can be the Zipf's law, well known in linguistics and texts analysis can be easily observed in the distribution of gene expressions in different samples of cancer tissues.

In recent years datasets with a large amount of cancer samples' data cancer are available, the most complete is The Cancer Genome Atlas (TCGA). From this dataset it is easy to get, for example, gene expression data from RNA sequencing experiments together with a lot of information about the sample itself.

If one studies the number of samples in which a gene is expressed above a certain threshold, the so called occurrence, it is easily verified that there are different kinds of genes. Some are present in the majority of samples, some others are present only in a subset of the whole dataset. This exact same behaviour can be found analysing words in a corpus of texts; some words, such as *the*, are present everywhere, other specific words are present only in texts regarding a certain subject. This suggests that there are similarities between a system of words and documents and a system of genes and samples.

Given a corpus of documents, they can be classified by their specific subject. In a similar way a set of samples can be classified, for example, by the tissue it comes from or by the type of the disease it is referred to.

The similarities between gene expression data and linguistics suggest the possibility to use topic modelling to classify data and separate samples and genes in different clusters. Topic modelling is a set of clustering algorithms in networks' theory. Given a set of words and documents, it describes documents as a mixture of topics. Topics are nothing but communities of words each with a given probability.

Purpose of this work is to build a bipartite network of genes and samples and use topic modelling to find communities. The goal is to separate samples depending on the site the tumour was and the disease type of the sample. Moreover it is possible to separate genes depending on their specific functions. In fact once a community structure of genes emerges, it is possible to run a hypergeometric test on the whole set in order to verify if they reveal some type of enrichment and to inspect their common properties.

The specific algorithm used in this work is particularly unique because it allows overlapping clusters; so it is possible to find genes belonging to different topics, this empowers a lot of new possibilities to investigate the network.

Furthermore a hierarchic approach can be used in finding topics, this let it possible to classify data at different layers. An ideal goal would be to separate healthy and diseased samples at the first layer, then separate by tissue, then by tumour type and so on.

Contents

Chapter 1

Introduction

In recent years the study of complex systems is becoming more interesting especially because some different systems can share interesting and fundamental properties. Network theory has proven to be a useful proxy to model and represent such complex systems.

This work wants to study and find universal statistical laws in different kind of biological systems. If one finds that two different systems share some important laws and data structure, therefore it is possible to use tool from different fields to study and gain information about each others. In particular two datasets containing information about some human healthy and diseased tissues will be analysed. This data come from biological experiments of RNA sequencing.

The ultimate goal of this work would be to study, develop and build machine learning's methods able to discriminate healthy and diseased tissues. Once diseased tissue are found, the next goal is to separate cancer types and ultimately sub-types, which is not always easy clinically.

The methods to gain this goal are derived firstly from linguistics, in particular a topic model approach will be widely described.

In chapter 2 I will describe the datasets used and introduce some basic biological properties of these datasets. In particular I'll use two datasets of gene expression data from diseased tissues and healthy tissues.

In chapter 3 I will describe the basics of component systems and give some basic mathematical definitions of quantities useful in general. This chapter refers in particular to the so called component systems.

In chapter 4 I will represent the gene expression from one sample from TCGA with respect to the genes' rank, one can easily obtain a Zipf's law. This law is well-known and in-depth studied in linguistics, demonstrating that different sources of data (genomic and linguistics) can share some statistical properties.

Demonstrated that linguistics and biological data share some laws in section 5 I will use topic modelling to perform network analysis on datasets. Using topic modelling one would find the inner structure of the samples. One would find clusters such that all samples in a cluster share the tissue and tumour type. As far as a document can contain a mixture of similar topics a single tumour can be very heterogeneous.

In chapter 6 I will discuss the results and the future developments

Many methods of the pipeline was written in C++ using openMP and Boost [1] are available at https://github.com/fvalle1/tacos. During this work I used different python libraries such as pandas [2], scipy [3], numpy [4] and matplotlib [5]. Some analysis required tensorflow [6] and pySpark [7]. The topic modelling stochastic block modelling minimization functions are implemented in the graph-tool library [8]. The full work repository is on Github at http://github.com/fvalle1/master_thesis.

Chapter 2

Data presentation

2.1 Dataset

The goal of [9] [10] [11] [12]

2.2 RNA-Sequencing

Data come from a RNA-Sequencing [13] experiments.

RNA-Sequencing data provide a unique snapshot of the transcriptomic status of the disease and look at an unbiased population of transcripts that allows the identification of novel transcripts, fusion transcripts and non-coding RNAs that could be undetected with different technologies.

Briefly, long RNAs are first converted into a library of cDNA fragments through either RNA fragmentation or DNA fragmentation (see main text). Sequencing adaptors (blue) are subsequently added to each cDNA fragment and a short sequence is obtained from each cDNA using high-throughput sequencing technology. The resulting sequence reads are aligned with the reference genome or transcriptome, and classified as three types: exonic reads, junction reads and poly(A) end-reads. These three types are used to generate a base-resolution expression profile for each gene, as illustrated at the bottom; a yeast ORF with one intron is shown.

The general steps to prepare a complementary DNA (cDNA) library for sequencing are, in general:

- RNA Isolation: RNA is isolated from tissue and the amount of genomic DNA is reduced
- RNA selection/depletion: To analyze signals of interest, the isolated RNA can either be kept as is or filtered for RNA that binds specific sequences. The non-coding RNA is removed because it represents over 90% of the RNA in a cell, which if kept would drown out other data in the transcriptome
- cDNA synthesis: RNA is reverse transcribed to cDNA (DNA sequencing tecnology is more mature). Fragmentation and size selection are performed to purify

sequences that are the appropriate length for the sequencing machine. Fragmentation is followed by size selection, where either small sequences are removed or a tight range of sequence lengths are selected. Because small RNAs like miRNAs are lost, these are analyzed independently. The cDNA for each experiment can be indexed with a hexamer or octamer barcode, so that these experiments can be pooled into a single lane for multiplexed sequencing.

In order to collect Gene expression data is sufficient to count how many reads are mapped to a specific exon or gene.

Data was collected from TCGA[1] dataset at https://portal.gdc.cancer.gov [14].

The particular datatype considered was *Gene Expression Quantification*, with experimental strategy RNA-Sequencing. At the end the downloaded dataset consisted of:

- N = 60483 genes as **components**
- R = 10672 files as **realizations**

This type of data is just a small portion of all data available on the portal, this are the most useful data for this type of analysis.

As highlighted in [15] these data present a challange to clustering tools, because of both the relatively large number of samples and the complex structure created by the inclusion of many different tissues

Attemts were made from GTEx [16] which is a similar source of data from healty tissues. [17] tried to unify data from this two different sources and data are available from [18]. Anyway gene expression data were downloaded directly from GTEx v7[2]

2.2.1 normalization

Ususally gene expression data can be normalized in different ways

- Counts
- RPK
- FPKM
- FPKM-UQ

Counts correspond to raw data. Anyway longer genes may have much reads than smaller gene, so it can be useful to normalize this data.

RPK[3] solves this by dividing counts by gene length L,

$$RPK = \frac{counts}{L}$$

.

[1] The Cancer Genome Atlas

[2] https://gtexportal.org/home/datasets

[3] Reads Per Kilobase of transcript

FPKM[4] are provided. FPKM calculation normalizes read count by dividing it by the gene length and the total number of reads mapped to protein-coding genes.

$$FPKM = \frac{RC_g * 10^9}{RC_{pc} * L} \tag{2.1}$$

where

- RC_g: Number of reads mapped to the gene
- RC_{pc}: Number of reads mapped to all protein-coding genes
- L: Length of the gene in base pairs

FPKM can be normalized to the 75th percentile read count value for the sample, in this case it is called FPKM-UQ. FPKM-UQ is obtained by:

$$FPKM - UQ = \frac{RC_g * 10^9}{RC_{g75} * L} \tag{2.2}$$

where

- RC_{g75}: 75th percentile read count value for genes in the sample

2.3 Clean data

2.3.1 Protein coding

The whole dataset contains infos on approximatly 60000 elements with different *ENSG* identifier. Only $\simeq$ 20000 of this are protein coding genes, using Ensemble[5] protein coding genes are selected.

2.3.2 Thresholds

In order to filter out noise, it is useful to put a threshold on the data. Considering data in $FPKM$ format, it is common opinion that values beleow 0.1 can be considered noise. Moreover data above 10^5 are trashed out, because the are syntom of some kind of errors during experiment.

Given this thresholds 3.1 becomes

$$o_i = \frac{\sum_{j=1}^{R} \theta(n_{ij} - 0.1) * \theta(10^5 - n_{ij})}{R} \tag{2.3}$$

[4] Fragments Per Kilobase of transcript per Million mapped reads

[5] https://ensemble.org

Chapter 3

Data structure

The data studied in this work can be represented as component systems. These component systems can be represented by a two dimensional matrix in which rows represent components and columns are the possible realizations buildable given subset of the components. The entries of this matrix are the number of the components on the row needed during the realization of the column. In figure 3.1 an example of this kind of matrices.

metti citazioni [19] [20] [21]

3.1 Component systems

$$
\begin{array}{cc}
 & \text{Realizations} \\
\text{Components} & \begin{pmatrix}
n_{11} & n_{12} & n_{13} & \dots & n_{1R} \\
n_{21} & n_{22} & n_{23} & \dots & n_{2R} \\
\vdots & \vdots & \vdots & \ddots & \vdots \\
n_{N1} & n_{N2} & n_{N3} & \dots & n_{NR}
\end{pmatrix}
\end{array}
$$

Figure 3.1: Structure of a matrix representing component systems with $i = 0 \dots N$ rows and $j = 0 \dots R$ columns

The most common example of such systems is a set of books, in this case one puts on the rows the words in the whole vocabulary and the books' titles on the columns; the entry that correspond to row i and column j is the number of times the word i appears in book j. The same happens if one considers Wikipedia's pages. Other examples are Lego® sets where components are the Lego® bricks and realizations Lego® packages and protein domains; all these were described and well studied in [19].

Given a matrix with N components on the rows and R realizations on the columns and relative abundances n_{ij} as the entries, it is interesting to study some quantities that are universal and general characteristics of component systems.

First of all, the **occurrence** of a component, defined as

$$o_i = \frac{\sum_{j=1}^{R}(1 - \delta_{n_{ij},0})}{R}, \tag{3.1}$$

is the fraction of realizations in which the component's abundance is not null. A component that is present in all the realizations has got $O_i = 1$, the ensemble of all components with $O_i = 1$ is known as **core**. Components with high ($\simeq 1$) occurrence are present in mostly all realisations of the datasets, in linguistics this components are articles. Components with low occurrence $\simeq 0$ are present only in a few realisations and are the most specific ones.

The sum across all columns is called **abundance** of a component and is defined as:

$$a_i = \sum_{j=1}^{R} n_{ij}; \tag{3.2}$$

dividing this by the global abundance

$$a = \sum_{i=1}^{N} a_i \tag{3.3}$$

naturally brings to the **frequency of a component** in the whole corpus

$$f_i = \frac{a_i}{\sum_{c=1}^{N} a_c}. \tag{3.4}$$

Dividing the abundance of a component by the sum of all abundances in a realisation gives the **frequency** of the component in that specific realization

$$f_{ij} = \frac{n_{ij}}{\sum_{c=1}^{N} n_{cj}}. \tag{3.5}$$

The sum of all abundances in the same realization

$$M_j = \sum_{c=1}^{N} n_{cj} \tag{3.6}$$

is called **size**.

It is expected that frequencies distribute according to the so called Zipf's law

$$f_i \propto r_i^{-\alpha} \tag{3.7}$$

where r is the rank: the position of a component when sorting all components by their frequencies in the whole dataset.

3.2 Universal laws in RNA-Seq

3.2.1 TCGA

Analysing TCGA dataset [14] the first interesting analysis is to plot the sorted abundance, this gives the so called Zipf's law. The analysis were made considering *Gene Expression Quantification* as data type, *Transcriptome Profiling* as data, *RNA-Seq* as experimental strategy, *HTSeq - Counts* or *HTSeq - FPKM* as workflow type. 5000

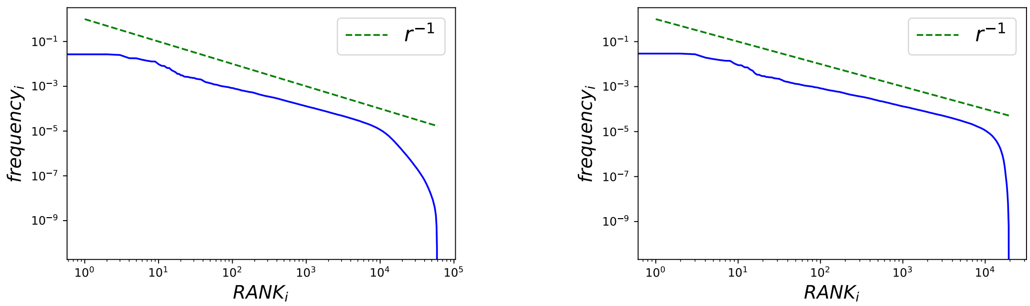

Figure 3.2: Zipf's law from FPKM normalised data. On the right considering only protein coding genes

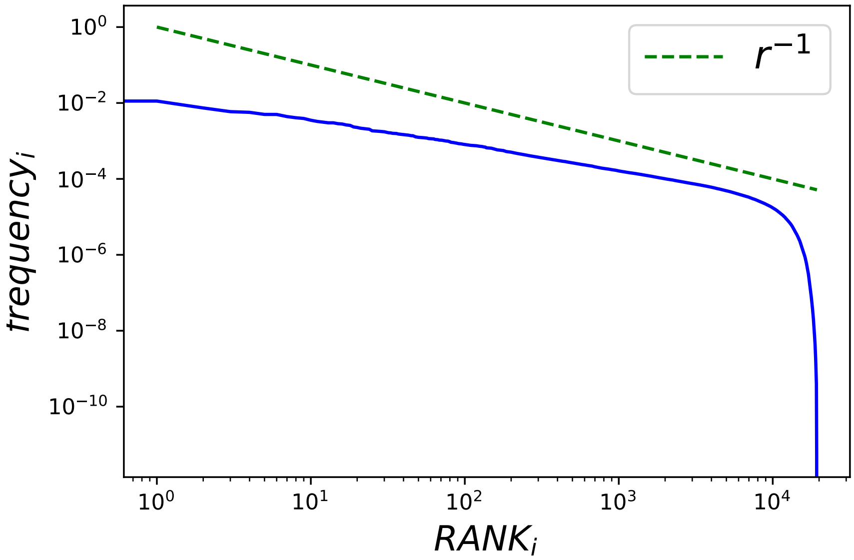

Figure 3.3: Zipf's law of protein coding genes considering counts

samples were downloaded and analysed. In figure 3.2 it is shown the frequency ranked plot. It is interesting that this kind of data distribute according a power law with exponent close to 1, this same behaviour can be found in completely different systems such as linguistics' ones [21]. Another interesting fact is that considering in the analysis also non-coding genes gives a double-scaled power law. This is due to the fact that non coding genes are also more specific and rare, so their frequencies are quite small compared to protein coding genes.

Changing normalisation and considering counts instead of FPKM, the result is quite similar. The power law is more flat, meaning that genes have more similar abundances in the whole dataset.

3.2.2 GTEx

A pretty similar analysis can be made on GTEx's [18] healthy samples. RNA sequencing raw counts data were download from file version *2016-01-15 v7 RNASeQCv1.1.8*. All ~ 11000 samples available were considered at this time.

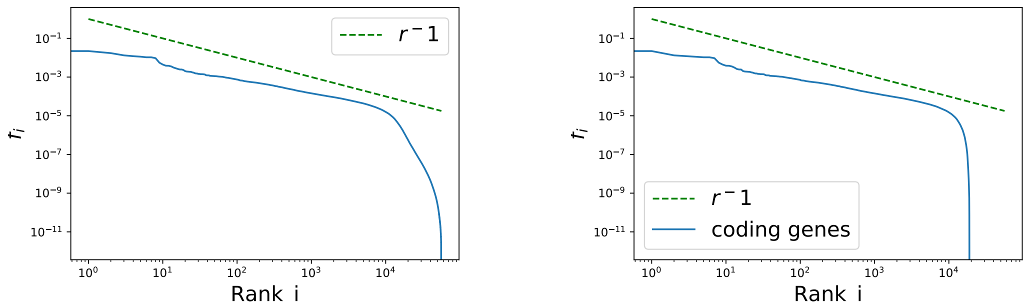

Figure 3.4: Zipf's law from GTEx count data. On the left all genes considered, on the right only protein coding ones

Not surprisingly in the GTEx dataset it is retrieved the same behaviour at this time. The power law with exponent $\simeq 1$ is found and considering non coding genes lead to a knee in the power law.

Going further in the analysis it is possible make an histogram of occurrences defined by 3.1, also known as Us.

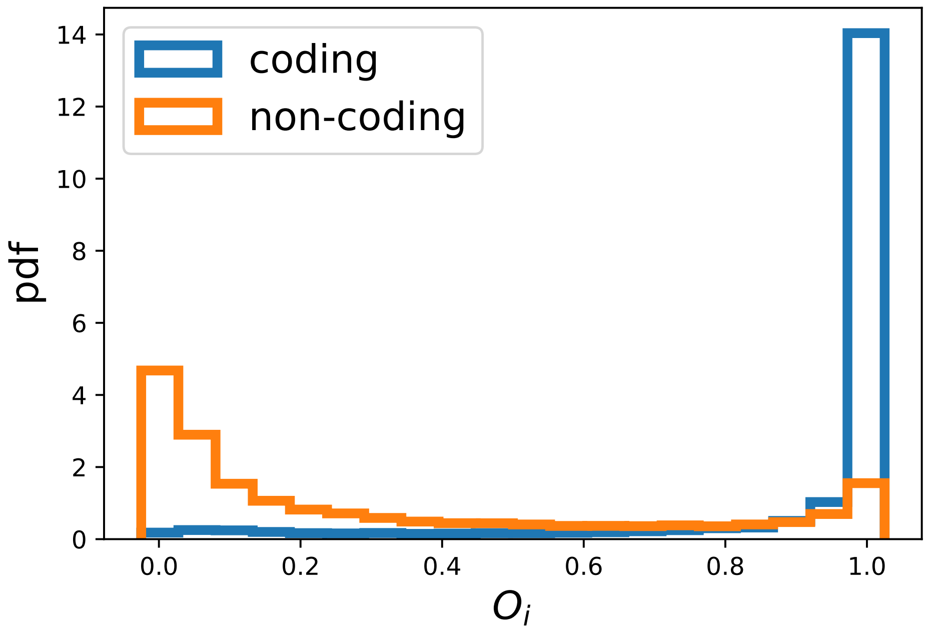

Figure 3.5: The histogram of the occurrences O_i

Also in this kind of analysis it is possible to see the different behaviour of coding and not coding genes. The protein coding genes express almost in every sample, so their occurrence is near to 1, non coding genes are more specific, so they are present only in a subset of the dataset and many of the have small occurrence. The same

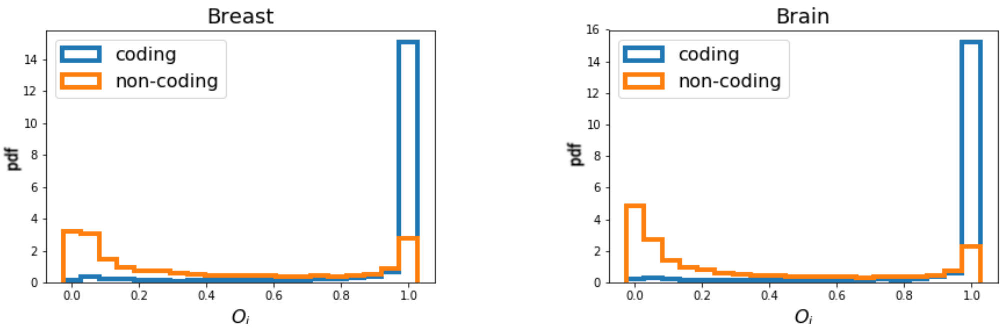

Figure 3.6: Same behaviour is observed looking at one tissue a time.

behaviour can be observed considering just all samples of a given tissue. In this case $O_i = 0$ means that the genes has a non zero expression in just one of the samples of the tissue considered; in other words if a gene never express in a tissue it is not considered when constructing these tissue specific U distributions.

From now on except were explicitly declared analysis will be made considering protein coding genes and counts with no normalisation.

3.3 Null model construction

The kind of data considered in this work comes from RNA Sequencing experiments. This experiments use wet biology methods to extract information from samples. If one imagines it exists an unknown function that describes the gene expression across the samples considered, what experimenters people do is to sample this function, picking up some genes.

In this section it is described a null model of sampling, this is useful to verify if the data distributions seen are just an effect of this experimental sample or if they carry some useful and interesting information.

As described in [22] a random matrix has to be created. This matrix is a collection of components and realizations exactly as 3.1. The values of abundances of each component in each realization n_{ij} are randomly assigned with a probability determined by the global abundance in the whole dataset 3.2. Values of each column are extracted until the size 3.6 is reached. Strictly speaking it is a multinomial process

$$P(n_i; M) = \frac{M!}{\prod_{i=1}^{N} n_i} \prod_{i=1}^{N} f_i^{n_i} \tag{3.8}$$

where n_i is the number of components with frequency f_i, being $f_i = \frac{a_i}{\sum_{i=1}^{N} a_i}$ as defined in 3.4.

Figure 3.7 shows an example of this, M components are picked up with respect to their frequency in the dataset. The most abundant components, which are also the

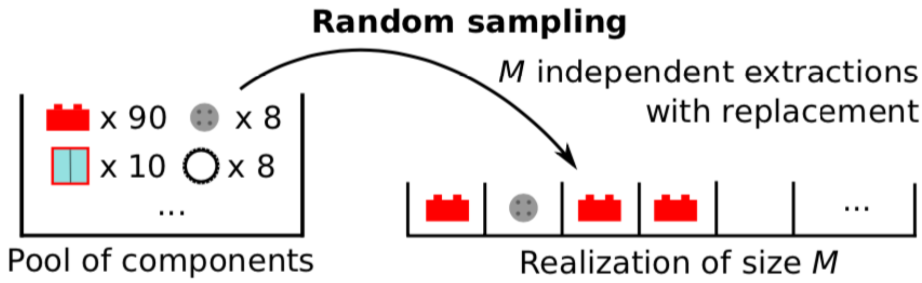

Figure 3.7: Random sampling of components to build a realization of size M

ones with higher frequency (frequency is nothing but the normalised abundance), have a greater probability to be picked up.

Using this construction on data of counts on both dataset, by definition the Zipf's law sampled are identical to the data's one. By construction the distribution of the

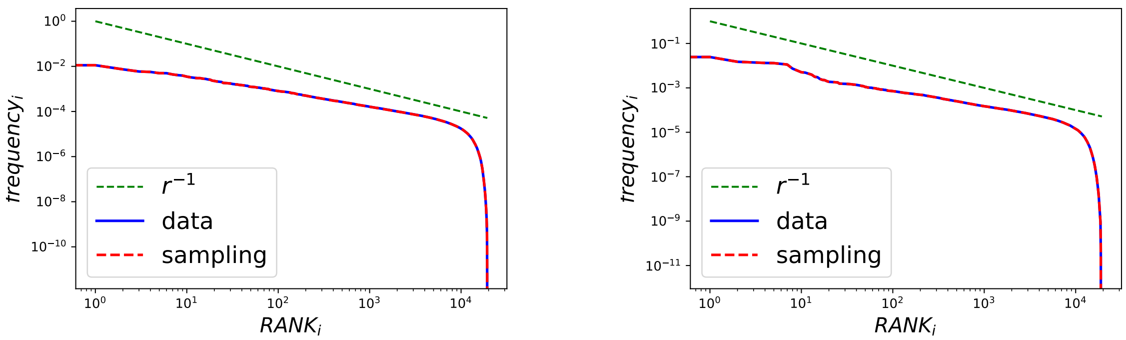

Figure 3.8: Zipf's law sampled; TCGA(left) and GTEx (right)

sizes of the sampling and of the data are identical.

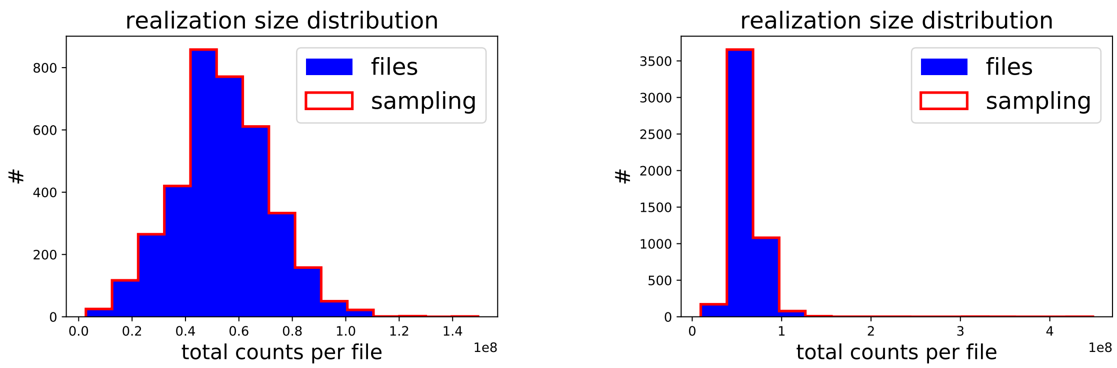

Figure 3.9: Distribution of sizes M; TCGA(left) and GTEx (right)

Looking at the Us, it is evident that data is different from sampling. This is a signal that the null model is not enough to explain the data matrices. In particular from figure 3.10 it is evident that the null model generate the matrices in a manner such that more components have high occurrence with respect to the original data. This can be easily explained, in fact in real world there are some genes that are highly expressed but only in a subset of the whole dataset; these genes are specific for certain type of samples. The null model gets the information the such genes are highly expressed from the abundance and so samples these quite often (components with high abundance have a greater chance to be picked up by the null model sampling).

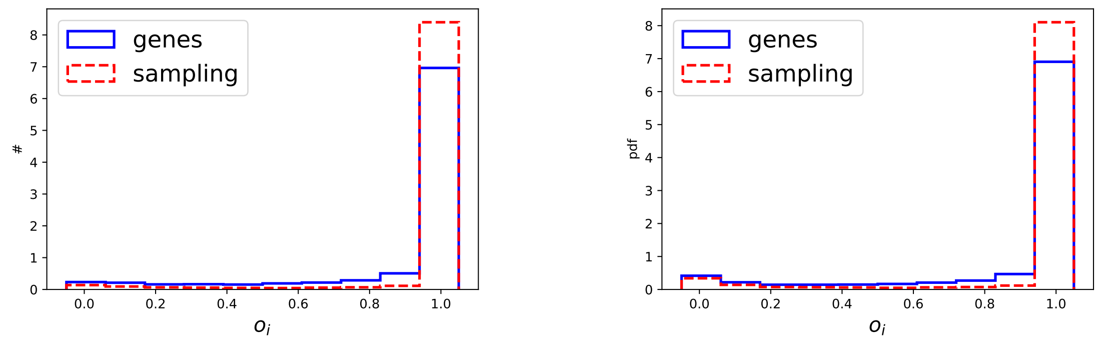

Figure 3.10: Occurrence distributions; TCGA(left) and GTEx (right)

Looking at the Heaps's law [23] , again the curves differ and the null model is not enough complete to explain the trend. In figure 3.11 the Heaps's law is presented compared to the one obtained by sampling, note that each data point share the abscissa with a sampling one (figures 3.9 are nothing but the histograms of the abscissas of 3.11). It happens that the sampling curve is above the data's one. This means that to build a sample of size M just by sampling it is necessary to use a greater number of different genes than the number of different genes actually expressed in nature. In other words in real world are expressed only the genes that are really useful in the sample, and this is not describable just by sampling. This fact is coherent with the fact that the Us differ. Another way to see this is looking at the histograms of the number of different

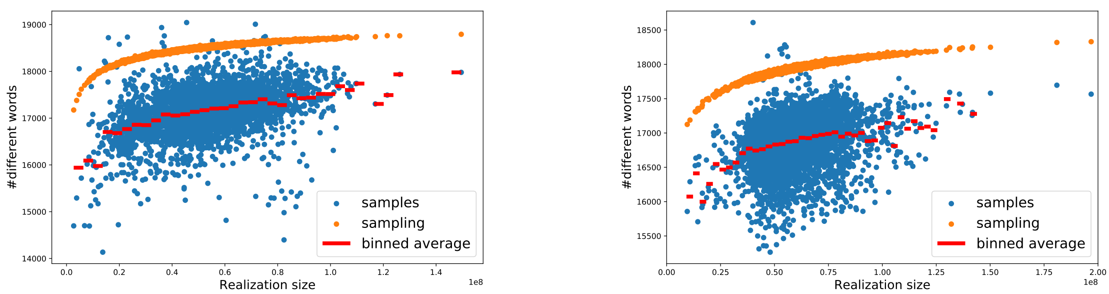

Figure 3.11: Heaps' law; TCGA(left) and GTEx (right)

genes expressed, actually the distribution of the 3.11 y axis. Figure 3.12 shows that these distributions are completely different if one looks at the data and at the samples.

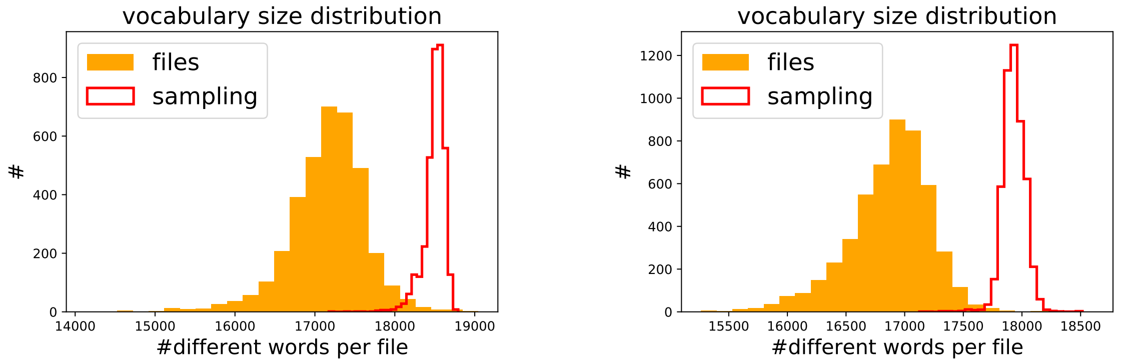

Figure 3.12: Occurrence distributions; TCGA(left) and GTEx (right)

3.4 Statistical laws differentiate by tissue

Observing the GTEx dataset of healthy samples it is possible to study how it is possible to see the tissue differentiation and how to study tissues' differences, [24] suggests the approach.

First of all could be interesting to study which is the fraction of transcript that can be explained by a certain number of genes. One can reduce the realisations to the ones that share the tissue. Than one estimates the average per each component (gene), at this point one has the average abundance of each gene in a tissue, dividing by the sum of all the components it is possible to obtain the fraction of the total counts in the tissue due to each gene. Sorting from greater to smaller and integrating (cumulative summing) one have the fraction of transcript due to $1, 2, 3\dots$ genes. This is plot in 3.13. Here, if a curve is steep it means that a few genes' counts represent a great fraction of the total. If a curve is smooth it means that many genes are necessary to describe the whole trascriptome for that particular tissue. This analisys shows that different tissues have a different complexity in terms of the number of genes necessary to build the trascriptome (in average). In figure 3.14 the same analisys is done for the sub-tissues of Brain, also this sub-type separate by tissue.

Coming back to the Zipf's law 3.7, it is now obvious that 3.13 represents nothing but the integral of the Zipf's law. So estimating the Zipf looking at a tissue a time, it is evident that each tissue has its particular slope. The steeper the Zipf the simplest is the tissue: the transcript can be described with a few genes. In figure 3.15 the tissue with an extreme behaviour.

The point where the 3.13 reaches 1 corresponds to the total number of genes expressed, the remaining ones have a 0 expression and do not contribute to the transcript. This can be visualised again with the Heaps' law. In figure 3.16 it is evident that there is some kind of tissue differentiation even when looking at the Heaps' law.

All these analysis suggest that there must be a sort of hidden structure in the data that is somehow related with the tissue each sample comes from. In particular there are many different Zipf's laws hidden behind the data and each sample is build looking at one of these a time. Also given two samples with a similar size, it happens that the number of genes necessary to build that realisation is not always the same (shown by Heaps' law) and it is somehow related to the tissue of the sample.

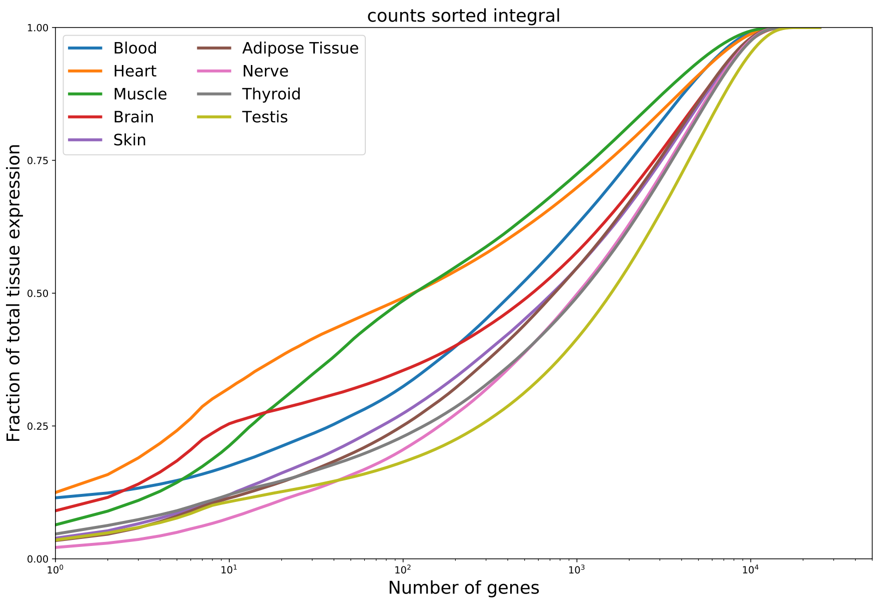

Figure 3.13: The integral of the sorted abundances for each tissue

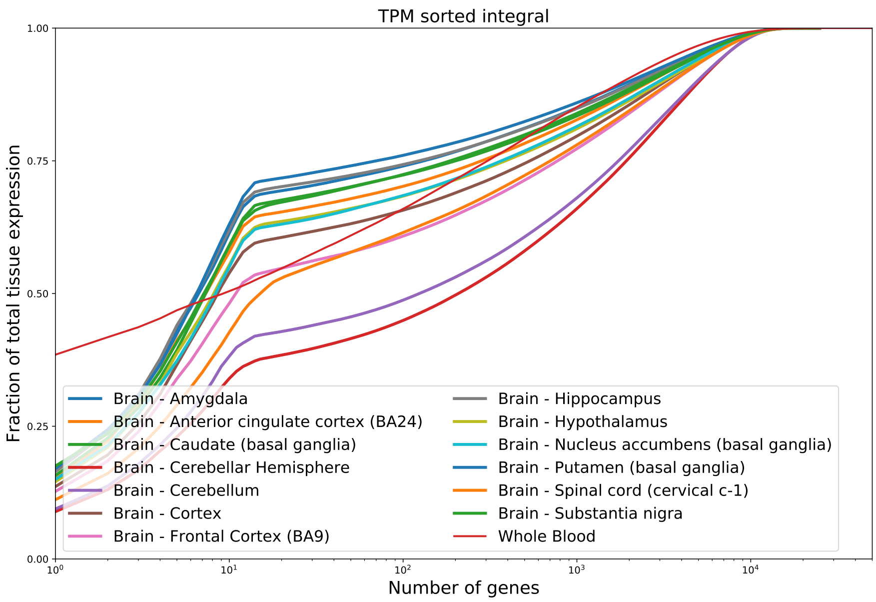

Figure 3.14: The integral of the sorted abundances for sub-types of Brain. This is done using TPM to avoid biases due to gene lengths. Blood is plotted for reference.

In conclusion, some interesting laws were found that some statistical.
...

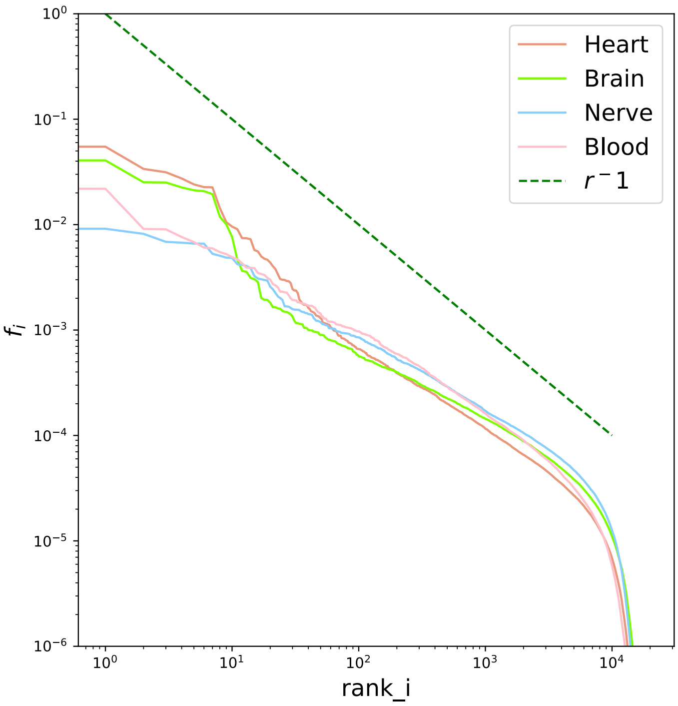

Figure 3.15: The integral of the sorted abundances for each tissue

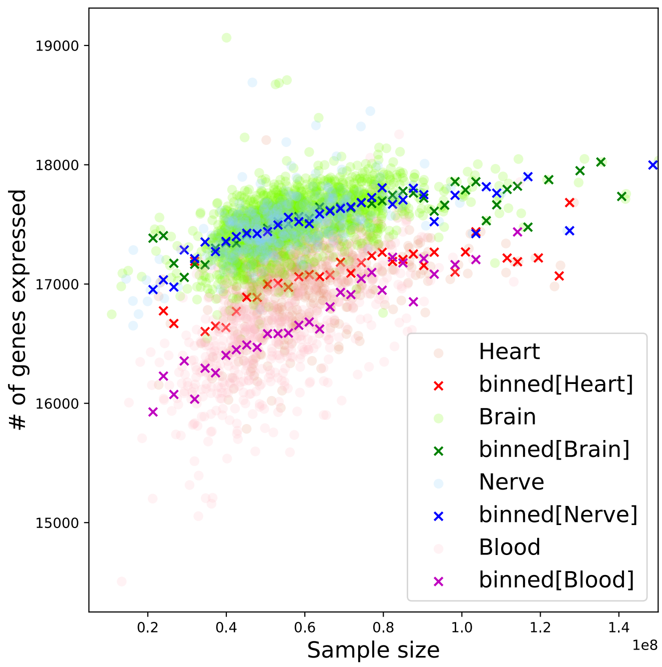

Figure 3.16: The integral of the sorted abundances for each tissue

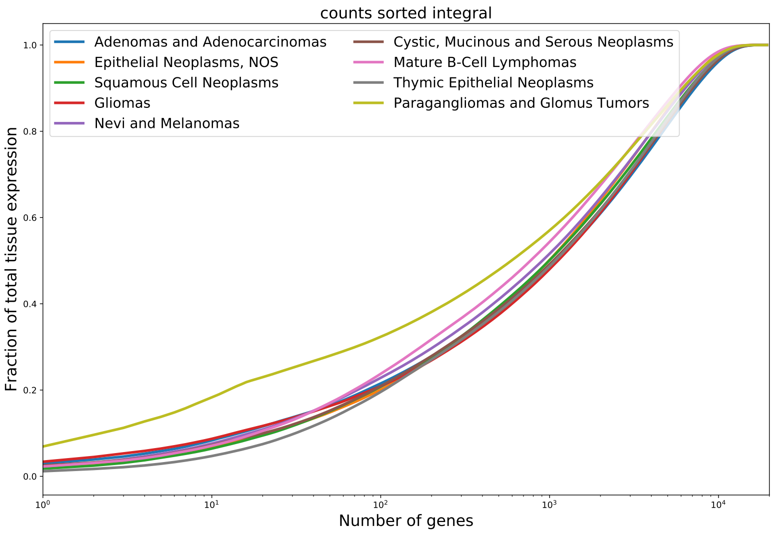

Figure 3.17: The integral of the sorted abundances for each tissue

Chapter 4

Scaling laws

One of the goals of this work is to search, reveal, study and use universal laws in bulk gene expression data . As in chapter 3 approaches from different field of science are considered at this point.

In can be interesting to study the behaviour of the gene expression across samples.

4.1 Scaling

gene expression across samples? gamma?

Given a matrix of components and realisations as 3.1 with expression entries n_{ij} it is possible to estimate the mean of a row $m_i = \langle n_{ij} \rangle_j$ and its variance $\sigma_i^2 = \left\langle n_{ij}^2 \right\rangle_j - \langle n_{ij} \rangle_j^2$.

First of all it could be interesting to study the variance of expression σ^2_{counts} versus the average $\langle \text{counts} \rangle$ across tissues. In figure 4.3 the scatter plot of variance versus

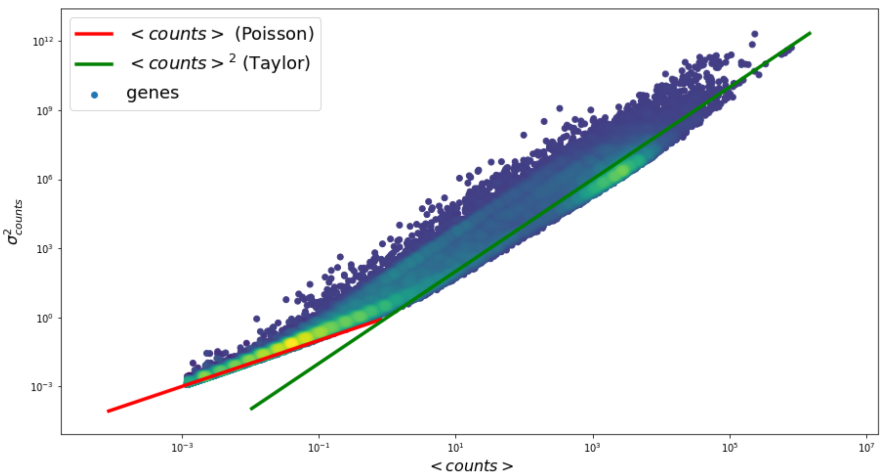

Figure 4.1: Variance versus average. In red the Poisson-like scaling, in green the Taylor-like scaling. All genes are considered

mean reveal some interesting facts. First of all it is evident that data have a double scaling behaviour: when the mean is small ($\lesssim 1$) data have a Poisson-like scaling ($\sigma^2_{\text{counts}} \sim \langle\text{counts}\rangle$), at higher means instead data have a quadratic scaling ($\sigma^2_{\text{counts}} \sim \langle\text{counts}\rangle^2$) known in ecology as Taylor's law [25]. This means that at low averages data behaviour is just due to the sampling experimental process, on the contrary the Taylor's law reveals the non trivial distribution across samples of the gene expression. Another interesting fact is that looking at the density of points (colours in figure 4.1) are evident two clouds of points, one at low averages, one at high averages. These correspond to coding and non coding genes, remembering section 3.2 these two kind of genes have a different behaviour: coding genes are highly expressed in the majority of the samples, non coding ones are less expressed (and so less sampled) in few samples.

A similar analysis, common in literature, is the analysis of the coefficient of variation squared $CV^2 = \frac{\sigma^2_{\text{counts}}}{\langle\text{counts}\rangle^2}$ represented in figure 4.2. The behaviour is complementary to

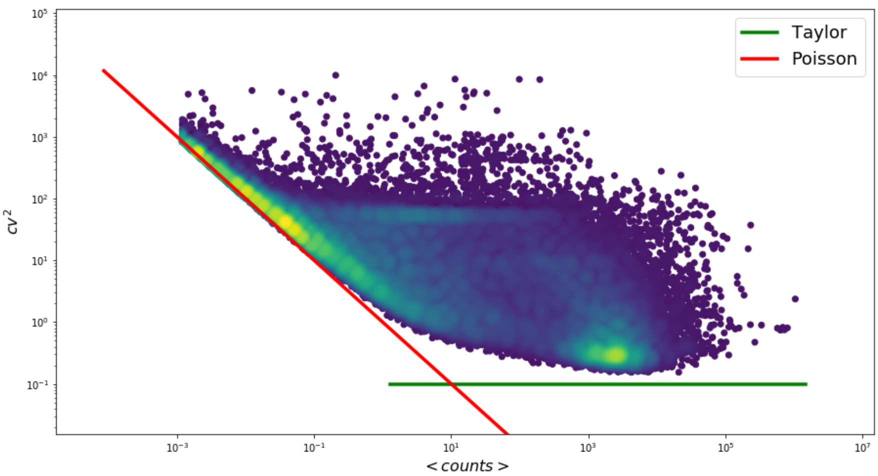

Figure 4.2: Coefficient of variation squared versus average. In red the Poisson-like scaling, in green the Taylor-like scaling

the above discussed double scaling and is quite common in literature looking at single cell RNA sequencing data [26]. Even looking at CV^2 it is evident the presence of the coding and non-coding clouds of points. The non coding genes are on the Poisson-like scaling, $\sigma^2_{\text{counts}} \sim \langle\text{counts}\rangle$ so $CV^2 = \frac{\sigma^2_{\text{counts}}}{\langle\text{counts}\rangle^2} \sim \frac{1}{\langle\text{counts}\rangle}$, otherwise the protein coding genes are on the Taylor-like curve $CV^2 = \frac{\sigma^2_{\text{counts}}}{\langle\text{counts}\rangle^2} \sim 1$.

Protein coding genes can be isolated and considered on their own. The same analysis confirms that the cloud of genes' points on the Taylor-like scaling are effective the protein coding genes. Following the sampling model of [22] sum up in section 3.3 the averages and variances can be estimated on null matrices. In figure 4.4 the comparison between real genes and sampling ones. The sampling has got a double scaling as well; this is quite interesting, it means that the global scaling is due to the Zipf distribution and the sizes distribution themselves, they are identical in data and sampling by definition. Moreover the sampling points draw a lower bound of the data, this encodes the

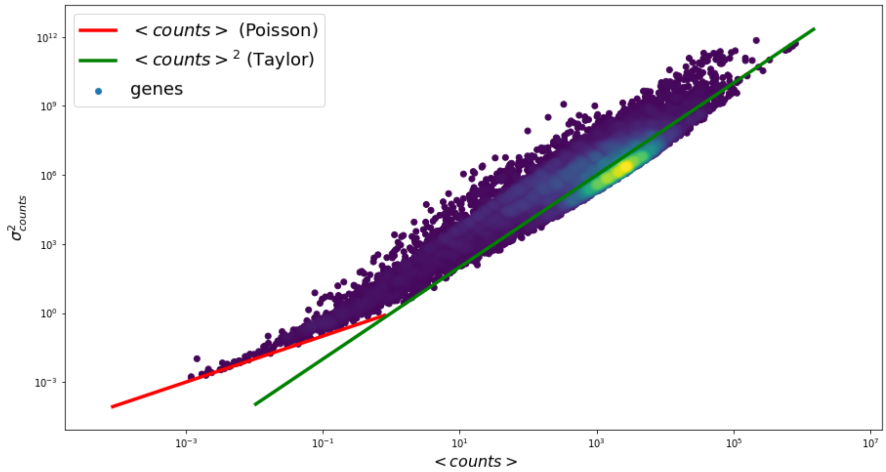

Figure 4.3: Variance versus average. In red the Poisson-like scaling, in green the Taylor-like scaling. Only protein coding genes are considered

information that the data are more variable (have higher variance) than just sampling, so there must be some biological information hidden that causes this over variable behaviour.

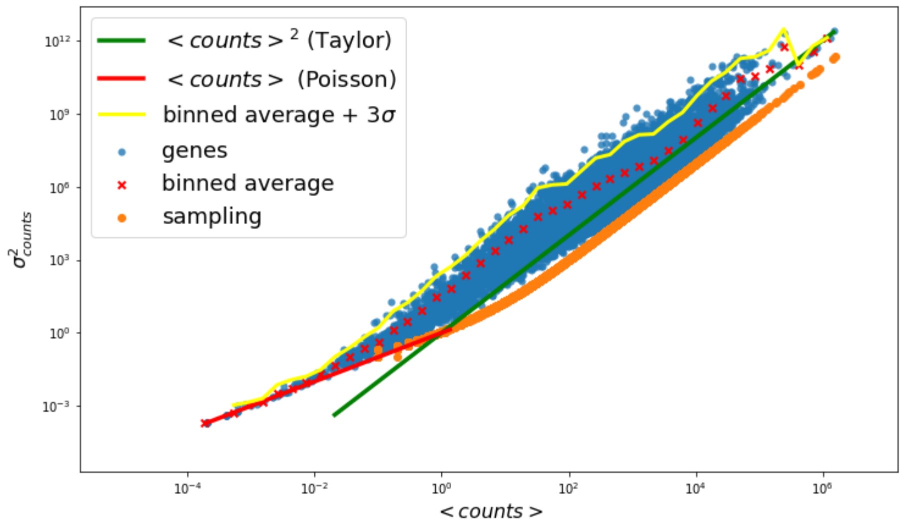

Figure 4.4: Variance versus average. In red the Poisson-like scaling, in green the Taylor-like scaling. In orange the sampling components. Only protein coding genes are considered

Again it is possible to analyse the CV^2, at this time considering only protein coding genes. Figure 4.2 confirms that the cloud of points near the Taylor-like scaling are the protein coding genes and a double scaling is seen once again.

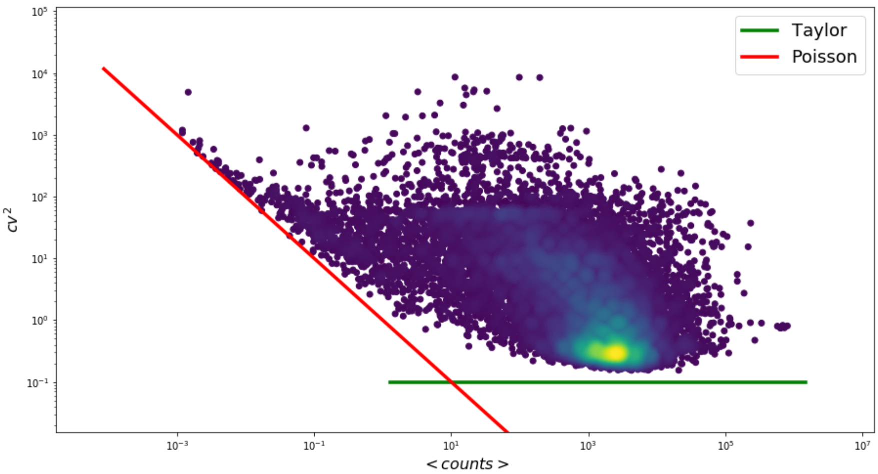

Figure 4.5: Variance versus occurrence

In figure 4.6 the same plot compared to the sampling points. The double scaling is evident also for the sampling points. Note that CV^2 has got a lower bound at 0 which corresponds to the less variable case if all expression are identical in all samples ($\sigma^2_{\mathrm{counts}}$) and an upper bound at $N-1$ with N the number of realisations and corresponds to the most variable case where a component express in only one realisation and is 0 elsewhere.

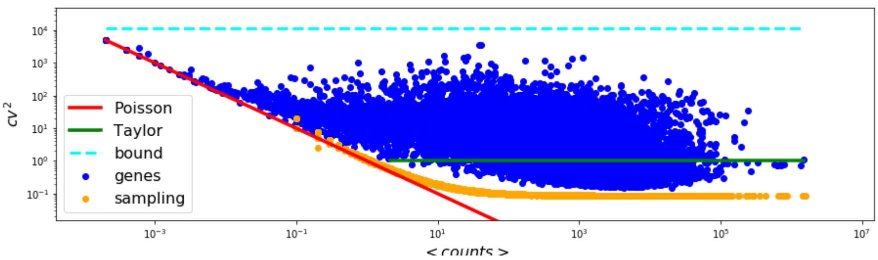

Figure 4.6: Caption

Finally the data have a double scaling when looking at their global variance across realisations, a Poisson-like where the sampling experimental process is more important and a Taylor-like where the complexity of the data emerges. Non coding genes have got low expression and are rare, protein coding genes, otherwise, express a lot and everywhere and carry more information following a double scaling. All genes are more variable than a sampling null model and this is the evidence that something interesting is hidden behind the data.

$< FPKM >$ **normalisation** One can be interested in finding genes that are expressed often, and what is the average expression of them. To manage this it is plotted the average expression $< FPKM >$ versus the number of samples in which that gene is expressed that is, considering the thresholds 2.3.2, $\Sigma_j \theta(FPKM_{ij} - 0, 1)\theta(10^5 - FPKM_{ij})$

4.1.1 Average versus occurrence

Another interesting analysis can be the relation between the occurrence and the average. In figure 4.7 it is shown the re sult, it is clear that there is a relation between occurrence and average, genes that express in more realisations (higher occurrence and right in the figure) have an higher average. Moreover doesn't exist genes that have high expression in few realisations; genes that are rare are also difficult to find so have a small average. Not e that the average has got a bound due to the fact that counts are integer numbers, so if, for example, one gene express in n of the R samples, it has occurrence $O_i = \frac{n}{R}$ and its average is at least $\langle \text{counts} \rangle = \frac{1*n}{R}$

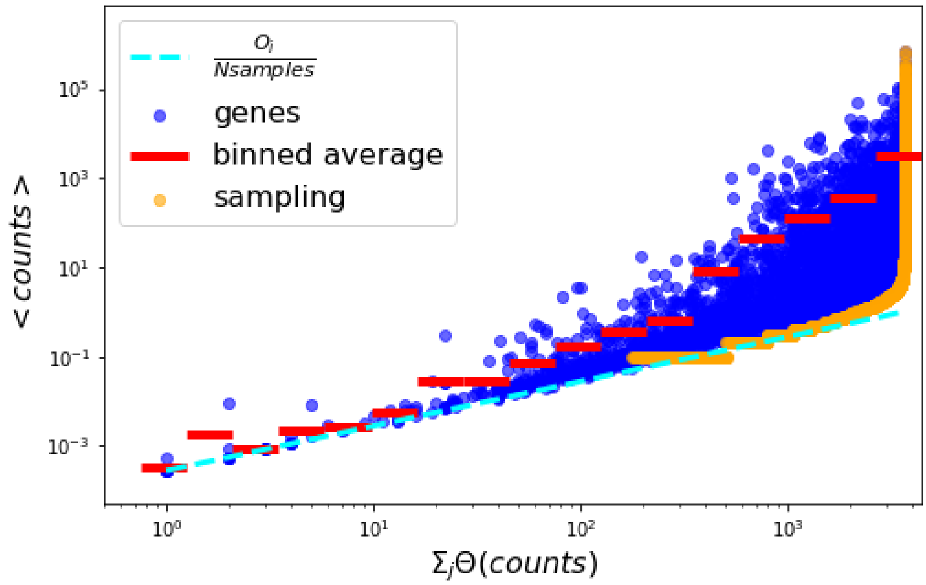

Figure 4.7: Relation between the occurrence of a gene and its average across realisations

4.1.2 Tissue differentiation

Per gene type scaling

Chapter 5

Topic modelling

Once extensively analyzed the structure of the dataset, the goal becomes to develop a machine learning method to learn the hidden structure of the data.

Remembering that in chapter 3 it emerged some kind of structure behind data, where each tissue seemed to be sampled by a different power law, a topic modelling approach it is here proposed.

The idea is that behind data there are hidden variables that describe the relationship between the genes and the samples. Let's call these variables topics. Firstly it is necessary to build a bipartite network of genes and samples, then nodes are linked considering the gene expression value in the dataset.

The output of this kind of model consists of sets of genes, the topics, with a probability distribution $P(gene|topic)$ and probability distributions of these topics inside each sample $P(topic|sample)$, both gives the relation between a *sample* and a *gene*.

In this work it is used an innovative and recent approach to topic modelling, the algorithm was presented by [27] and extends the so called stochastic block models [28]. Topic modelling is being developed and studied to approach linguistics problems, so this algorithm was developed considering words and books as input, links represents the abundance of a word in a book. In chapter 3 was evident that there are many similarities between data considered in this work and linguistics' dataset. Referring to data used in this project **samples** will be the documents and **genes** will be the words. It is expected that topics represent some properties of samples due to the gene expression distribution in samples.

The ultimate goal would be to be able to separate healthy and diseased samples than separate and find well-known tumour types, then extend the actual knowledge and retrieve the tumour sub-types.

One of the advantages of this particular algorithm is that it is hierarchical, so it applies community detection at different layers. So the output has got different resolution, the extreme one is the separation, by definition, between samples and genes, at other layers it is possible to have few big clusters until the other extreme were the number of clusters is comparable with the number of nodes.

What the algorithm does is to run a sort of MonteCarlo simulation and find the best partition of the data. The probability that the hidden variables θ describe the

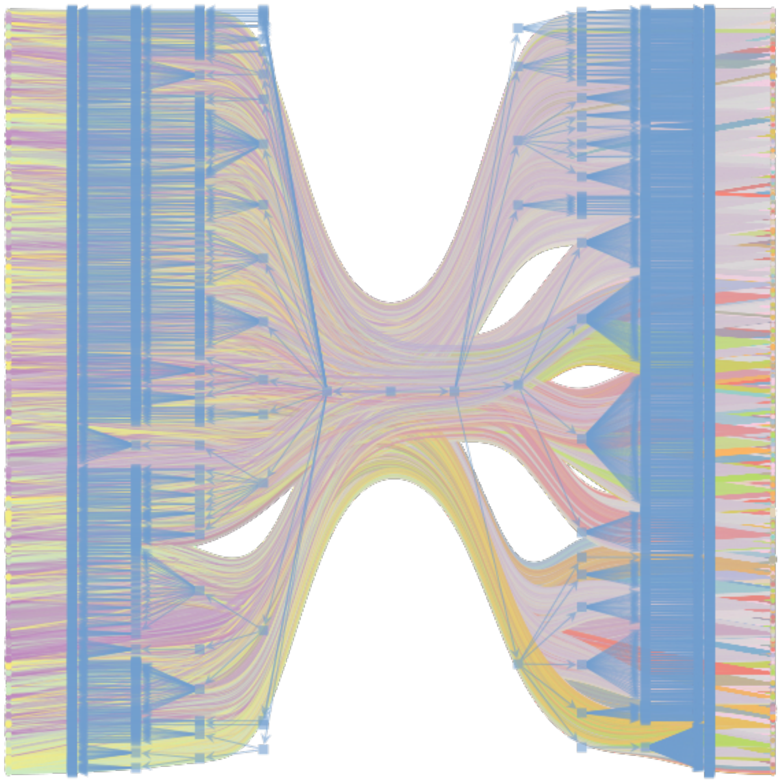

Figure 5.1: An example of a bipartite network. Samples are on the left, genes are on the right. Each link is weighted by gene expression value. On the left side, all nodes of the same colour are clusters of samples. On the right side, all nodes with the same colour are set of genes, also known as topics.
Blue lines represent the cluster structure, each blue square is a set of nodes, lines delineate the hierarchical structure.
It is clear in the middle the network separation in genes and samples.

data G $P(\theta|G)$ can be written as a likelihood times a prior probability as

$$P(\theta|G) = \frac{P(G|\theta)\overbrace{P(\theta)}^{prior}}{\underbrace{P(G)}_{\sum_\theta P(G|\theta)P(\theta)}}.$$

It is possible to define a description length

$$\Sigma = -lnP(G|\theta) - lnP(\theta),$$

so that $P(\theta|G) \propto \exp -\Sigma$. Moreover, the likelihood $P(G|\theta)$, can be written as $\frac{1}{\Omega}$ where Ω is the number of possibles realisations given θ. This can be represented as a microcanonical ensemble with entropy $S = Ln\,(\Omega)$. Note that $\Sigma = S - lnP(\theta)$. According to [29] entropy S can be written as

$$S = \frac{1}{2}\Sigma_{r,s} n_r n_s H\left(\frac{e_{rs}}{n_r n_s}\right),$$

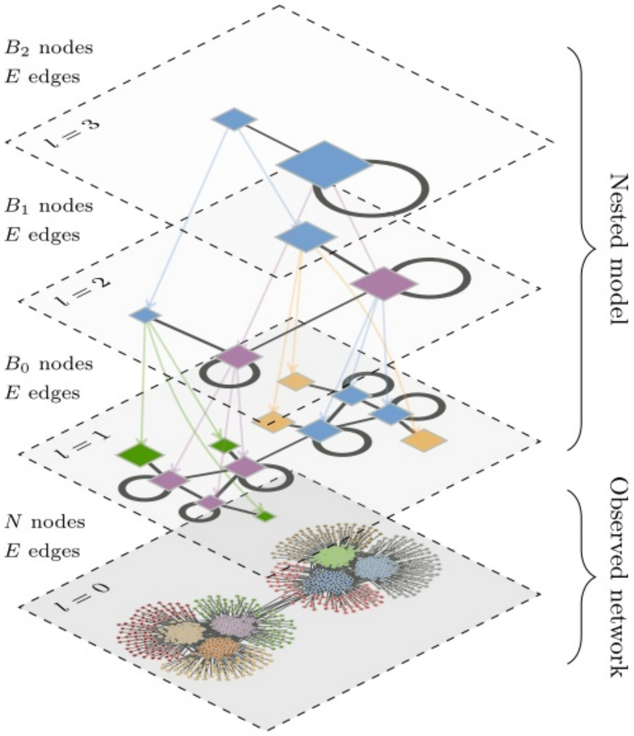

Figure 5.2: Hierarchical structure

where n_r is the number of nodes in block r, e_{rs} the number of links between nodes of group r and group s and H is the Shannon entropy $H(X) = xLog_2(x)+(1-x)Log_2(1-x)$. Note that S is minimal if $\frac{e_{rs}}{n_r n_s}$ is close to zero, r and s are two completely separated blocks or if it is close to 1, r and s are groups with many connections; this allows to find groups with nodes very disconnected or topic and clusters with a lot of connections. The algorithm tries to minimise S, so that Σ is minimised, so $\exp -\Sigma$ is maximised, but this is $P(\theta|G)$ that is the required probability to maximise.

The MonteCarlo works in a few steps:

- a node i is chosen
- the group of i is called r
- a node j is chosen from i's neighbours, the group of j is called t
- a random group s is selected
- move of node i to group s is accepted with probability $P(r \to s|t) = \frac{e_{ts}+\epsilon}{e_t+\epsilon B}$
- if s is not accepted, a random edge e is chosen from group t and node i is assigned to the endpoint of e which is not in t

in figure 5.3 an example of these steps. Once the model run it is possible to estimate

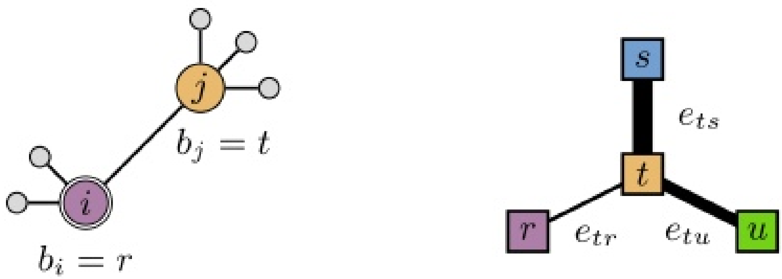

Figure 5.3: Left: Local neighbourhood of node i belonging to block r, and a randomly chosen neighbour j belonging to block t. Right: Block multi graph, indicating the number of edges between blocks, represented as the edge thickness. In this example, the attempted move $bi \to s$ is made with a larger probability than either $bi \to u$ or $bi \to r$ (no movement), since $e_{ts} > e_{tu}$ and $e_{ts} > e_{tr}$.

the probability distribution of words inside a topic

$$P(w|t_w) = \frac{\#\text{ of edges on } w \text{ to } t_w}{\#\text{ of edges on } t_w}$$

and the topic distribution inside a document

$$P(t_w|d) = \frac{\#\text{ of edges on } d \text{ from } t_w}{\#\text{ of edges on } d}$$

In the case of overlapping partitions, the presence of a word in a topic is not trivial and can be estimated as

$$P(t_w|w) = \frac{\#\text{ of edges on } w \text{ to } t_w}{\#\text{ of edges on } w}$$

or the presence of a document in a cluster

$$P(t_d|d) = \frac{\#\text{ of edges on } d \text{ to } t_d}{\#\text{ of edges on } d}$$

See appendix A for detailed analysis of the math behind the algorithm and https://cloud.docker.com/repository/docker/fvalle01/hsbm for the extension of [27] to non linguistics component systems datasets.

5.1 Metrics and benchmarks

Before running topic modelling, it is useful to define some metrics to test and benchmark the model. In particular the model search sets on the two sides of the network the one containing samples and the one containing genes. Samples are extracted from datasets where much metadata are available, some of these metadata labels will be used to benchmark the model. To study genes enrichment test are necessary.

Looking at the samples side of the network, the outputs are sets of samples, the clusters. One can state the model works if all, or at least the majority, of samples in the same cluster share some label. Here the tissue is considered as the main label.

Note that this work's model is a non supervised one, but a ground truth is available from metadata. So every sample has a certain probability to have a certain property (the true tissue label), let's call this $P(C)$ and a certain probability of being in a cluster (model's output), let's call this $P(K)$. It is possible to define some quantities, the homogeneity

$$h = 1 - \frac{H(C|K)}{H(C)} \tag{5.1}$$

defining the entropy

$$H(C|K) = \sum_{c \in \text{tissues}, k \in \text{clusters}} \frac{n_{ck}}{N} Log\left(\frac{n_{ck}}{n_k}\right) \tag{5.2}$$

where n_{ck} is the number of nodes of type c in cluster k, N the number of nodes and n_k the number of nodes in cluster k. It is evident that if all nodes inside cluster k are of the same type c $n_{ck} = n_k$, $H(C|K) = 0$ and $h = 1$, it is actually a complete homogeneous situation.

Another quantity can be defined and it is completeness:

$$c = 1 - \frac{H(K|C)}{H(K)}, \tag{5.3}$$

$H(K|C)$ is defined in the same way as 5.2. Completeness measures how well nodes of the same type are distributed in the same cluster.

Ideally one wants a method which output is both homogeneous and complete. So it is possible to define the V-measure as the harmonic average of the two:

$$\mathrm{V-measure} = 2\frac{hc}{h+c}, \tag{5.4}$$

which is actually the normalized mutual information between $P(C)$ and $P(K)$ [30]. Please refer to appendix B to the detailed math. In figure 5.4 an example of the V-measure score estimated at the different layers of the hierarchy; note that the number of clusters increases going deeper in the hierarchy. In the same figure homogeneity and completeness are reported, note that with few clusters the situation is more complete, but when the number of clusters increases completeness goes down and homogeneity increase.

In the next sections will be studied also the maximum fraction of label in the same cluster defined as

$$max_{c \in k} \frac{n_{ck}}{n_k}.$$

Also the number of different labels in the same cluster will be studied.

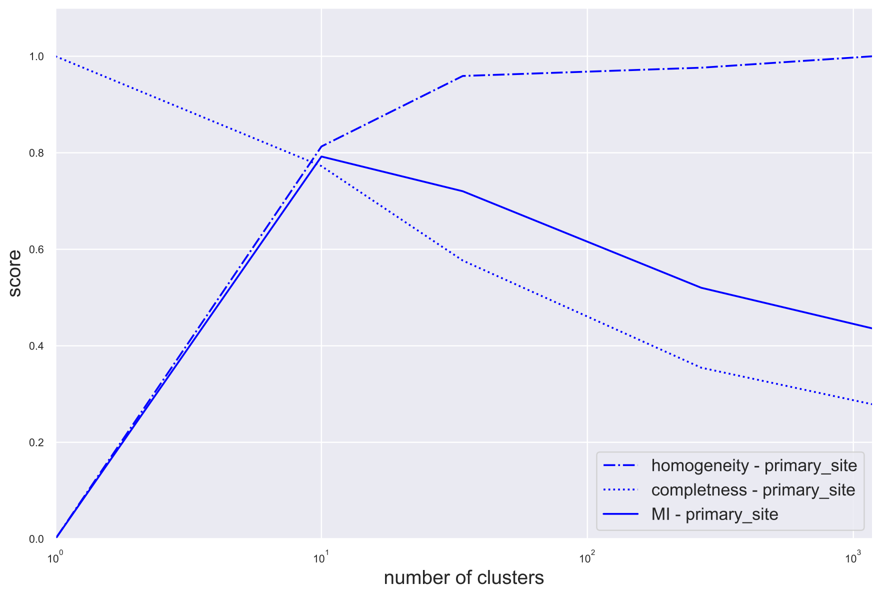

Figure 5.4: Score across hierarchy. The V-measure or normalized mutual information MI is the harmonic average between homogeneity and completeness.

5.1.1 Hierarchical clustering

Hierarchical clustering is a general family of clustering algorithms that builds nested clusters by merging or splitting them successively. This hierarchy of clusters can be represented as a tree (or dendrogram). The root of the tree is the unique cluster that gathers all the samples, the leaves being the clusters with only one sample. To perform hierarchical clustering the AgglomerativeClustering function from scikit-learn was used. Note that this approach was applied just to samples, nothing was done to classify genes. In this case genes are only dimensions in which samples are represented.

The AgglomerativeClustering object performs a hierarchical clustering using a bottom up approach: each observation starts in its cluster, and clusters are successively merged. The linkage criterium determines the metric used for the merging strategy. First of all, distances between all elements are estimated; in this work was used standard euclidean distance. Then elements are merged using a linkage criterion; in this work standard Ward linkage was used. The Ward linkage minimizes the sum of squared differences between the distances. It is actually a variance-minimizing approach. Here the specific setting used in this work.

```
from sklearn.cluster import AgglomerativeClustering
AgglomerativeClustering(
    affinity='euclidean',
    compute_full_tree='auto',
    linkage='ward',
    n_clusters=x,
    )
```

In figure 5.5 an example of a hierarchical clustering. Note that nodes with short distance are linked firstly.

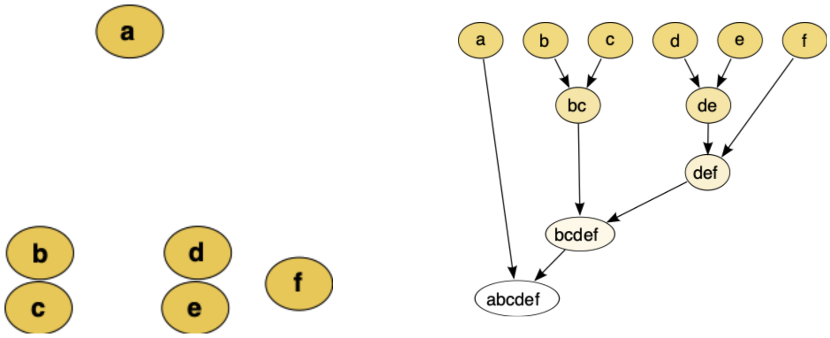

Figure 5.5: Example of hierarchical clustering

5.1.2 LDA

Latent Dirichlet Allocation is another approach to topic models. It has got more restrictive priors and needs some parameters to be set. It uses some different methods to maximize the posterior probability to observe some latent variables given the data. As well described in [10] LDA is a generative model and can be summarised as follows:

- for each topic k generate $\beta_k \sim \text{Dirichlet}(\bullet|\eta)$
- for each document d generate $\theta_d \sim \text{Dirichlet}(\bullet|\alpha)$
- for each word in d
  - generate $z \sim \text{Multinomial}(\bullet|\theta_d)$
  - generate $w \sim \text{Multinomial}(\bullet|\beta)$

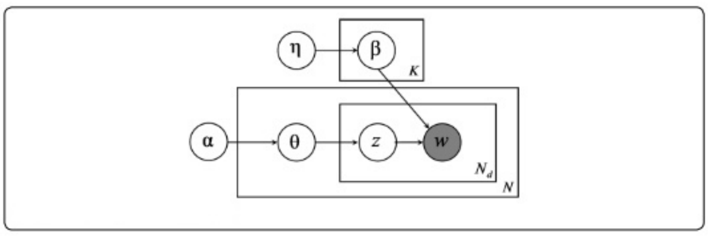

Figure 5.6: LAD scheme

this process is summarized in figure 5.6. These steps are useful to maximize the posterior probability

$$P(w, z, \beta, \theta|\alpha, \eta) = \prod_{d=1}^{N} P(\theta_d|\alpha) \prod_{n=1}^{N_d} P(w_{dn}|z_{dn}, \beta)P(z_{dn}|\theta_d) \prod_{k=1}^{K} P(\beta_k|\eta) \tag{5.5}$$

where

- N is the number of documents
- K is the number of topics as set by the user
- w are words
- N_d is the number of words in document d
- α and η are parameters of the model (usually $\eta = 0.01$ and $\alpha = 50/K$)
- $P(\theta|\alpha)$ and $P(\beta|\eta)$ are Dirichlet distributions

When β, θ and z are estimated, the outputs are the topic distribution in documents $P(z|d)$ and the word distribution in topics $P(w|z)$.

5.2 Pre-process

To make the algorithm faster, it could be useful to do a pre-processing of the data. Different approaches were tested, all of them involving the quantities defined in 3. The goal is to identify components which are able to best separate the realizations.

Low occurrence genes were selected firstly to approach topic modelling. A 0.5 threshold was set on occurrence. This method selects genes that appears (have expression greater than zero) only in less than half samples. This approach has some limitations, for instance it doesn't consider genes that appear everywhere (with occurrence $\simeq 1$) but changes their behaviour across realisations.

tf-idf (term frequency–inverse document frequency) should help. This approach doesn't take in account original expression values n_{ij}, but a transformed version

$$n_{ij}^{new} = \frac{n_{ij}}{M_j} \times (1 - Log\,(o_i))$$

which increases the importance of components with small occurrence o_i. This approach doesn't actually select components, which is still an issue.

Highly variable genes can be selected. This is done using the CV^2 analysis done in chapter 4. Plotting the coefficient of variation versus the mean for each component reveals which components have higher variance with respect to components which, on average, have a similar behaviour. Binned averages and variances were estimated, and only genes with a CV^2 over a σ greater than the bin's mean were considered. This method seems to select useful genes even if the binned average bound is quite noisy.

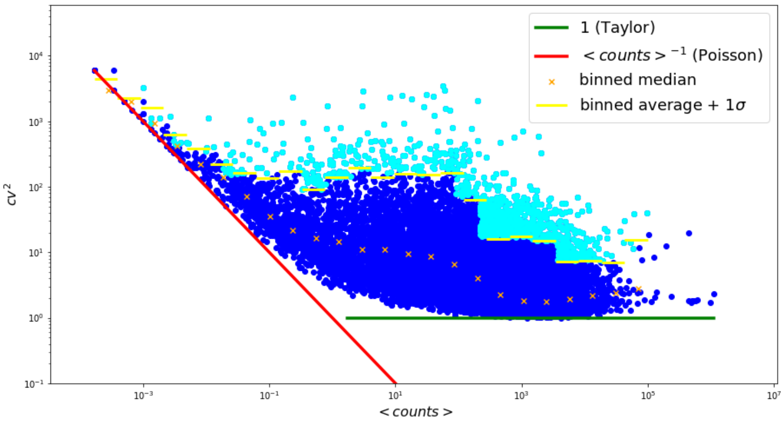

Figure 5.7: Highly variable genes

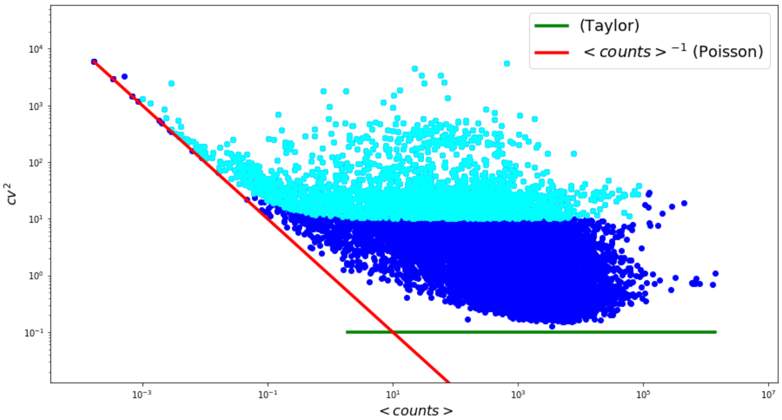

Figure 5.8: Genes distant from the boundaries

Distance from boundaries can be a similar and alternative method to select highly variable genes. In this case the bound is smooth and well defined. The distribution as discussed in 4 have a Poisson-like and a Taylor-like boundaries. So can be considered only components that are the most distant from these boundaries. Moreover this boundaries can be found with a simple null model, as shown in figure **??** the sampling model defines the lower bound of the data.

The last two approaches are the ones which lead to better results, in the following sections gene selection was done by getting only highly variables genes.

5.3 Run

5.3.1 Run on Gene Tissues Expression dataset

Once the model was tuned and adapted to RNA-Sequencing data, it was run on a subset of the GTEx dataset. A subset was chosen randomly in order to reduce the computing time needed. The analysis hereby described took about 2 days to be run on a 16 core CPU, 100GB memory facility. The great amount of memory is needed to temporary store the network configuration at each step of the Monte Carlo simulation.

First of all to rapidly have information about the interest of the oncoming result the metric above described were considered. In figure 5.9 it is represented the V-measure score versus the number of clusters found at different layers. The result is quite good,

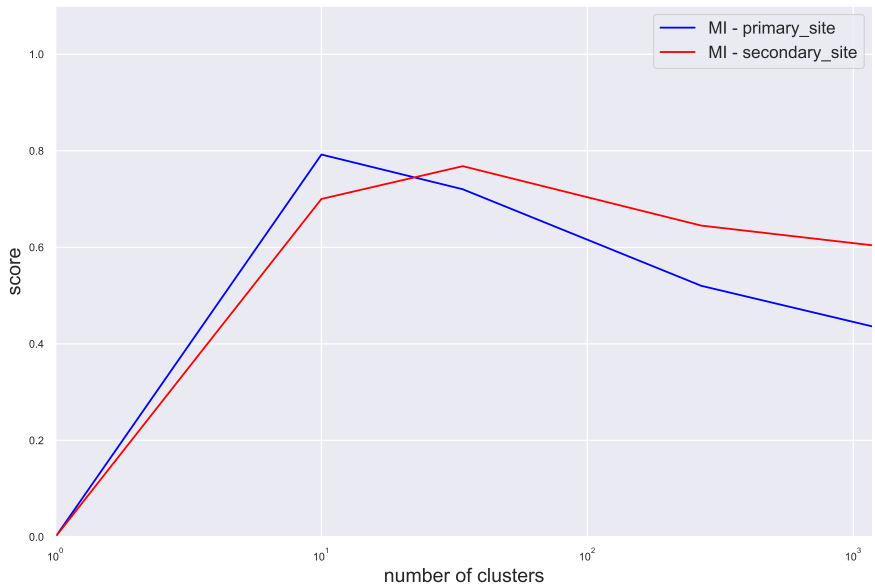

Figure 5.9: Scores across the hierarchy. The primary site and secondary site labels are compared.

the maximum score is over 0.8. Considering that, for example, [9] obtained a similar score analysing similar dataset considering just homogeneity, this can be considered a quite good result. A second interesting fact is that both the tissue label (primary site) and the sub-tissue label (secondary site) obtain such a good score, moreover the the secondary site score's peak is at a higher number of clusters coherently with the fact that there is a greater number of sub tissue labels. This score can be useful to extract the correct level of the hierarchy the consequent analysis should be made on.

In figure 5.10 the relation between the clusters at different layers it is evident.

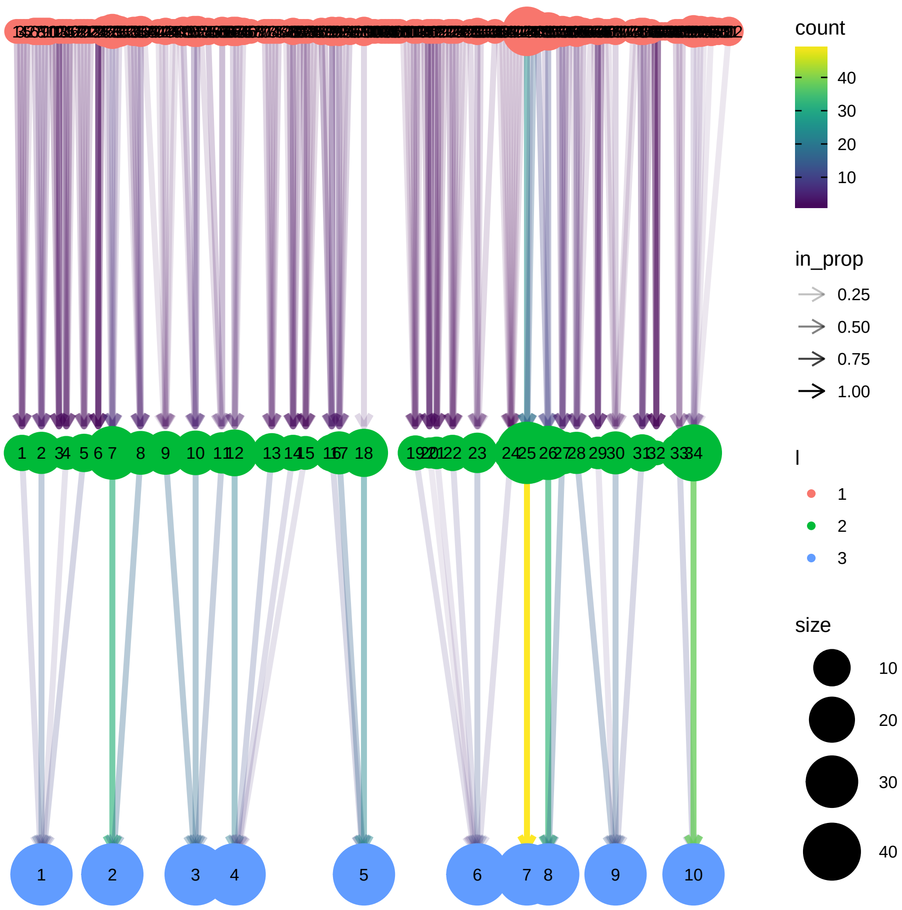

Figure 5.10: Hierarchy of the files' nodes.

In figure 5.11 each column is a cluster and each colour is a tissue of the dataset. It is evident that the majority of the tissue are identified: the first, second, fifth, sixth, eighth and tenth columns are fully and uniformly coloured of the same colour. These correspond to an identification of brain, blood, lung, testis and bladder. A

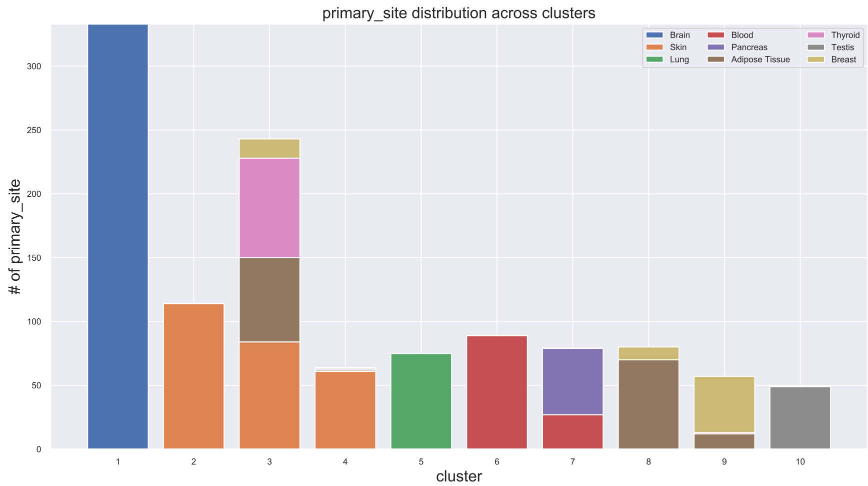

Figure 5.11: Clusters composition at the level of the hierarchy with higher score. Each column is a cluster, each colour is a label.

normalised representation of the same clusters the result is still quite interesting and the homogeneity of the clusters is more evident. Going deeper in the hierarchy and

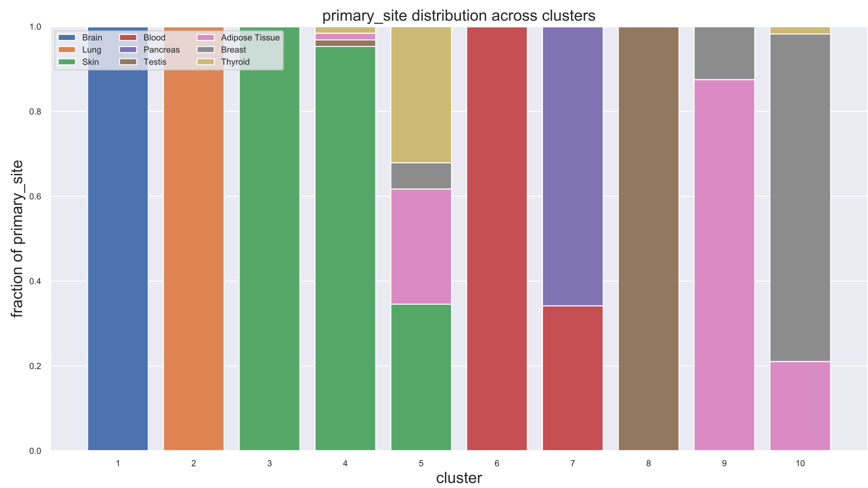

Figure 5.12: Normalised composition of clusters.

looking at a layer with more cluster the result, shown in figure 5.13, demonstrates that at this point all the tissues are separated and each cluster is full of nodes sharing the

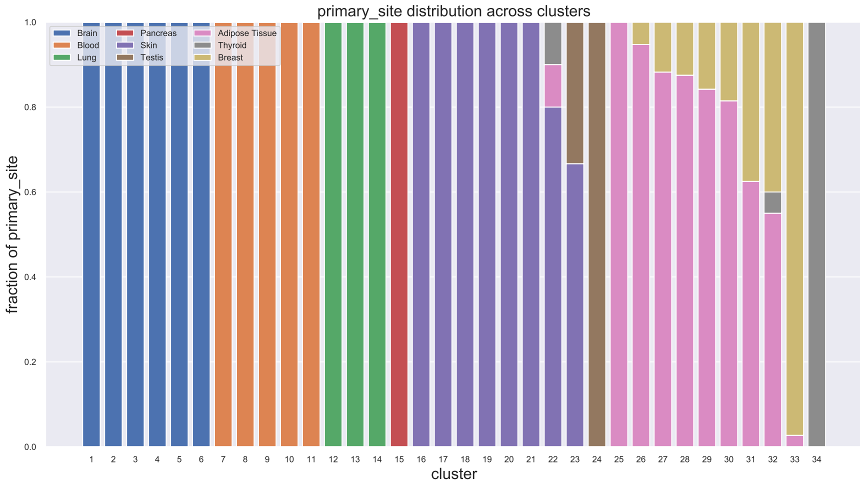

Figure 5.13: Normalised composition of clusters at a deeper level.

same tissue. Even looking at sub-tissues the results is quite good. It is not always easy to separate all the sub-parts of the brain, nevertheless, the cerebellum is well identified (column 13) and blood is distinguished in whole blood (columns 1-4) and lymphocytes (column 10).

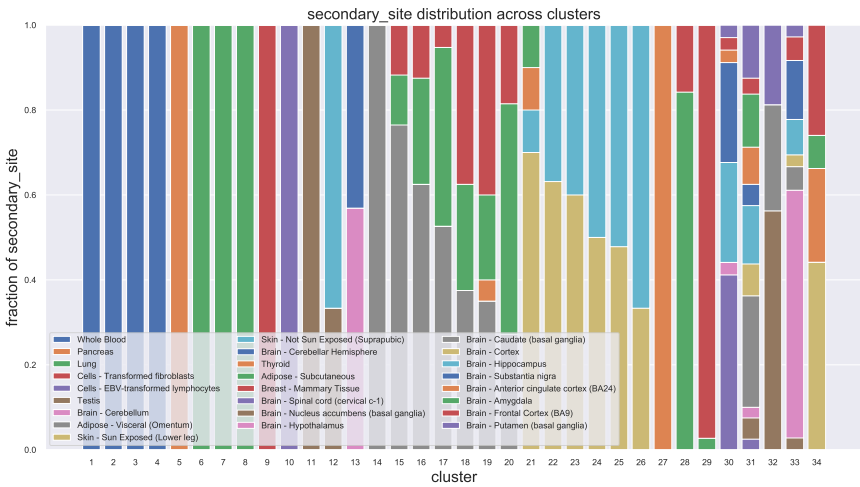

Figure 5.14: Normalised composition of clusters with respect to the secondary site sub-tissue labels.

5.3.2 Shuffling

A null model of cluster composition is necessary In order to be able to state that a result is better than expected. This was done by doing the same analysis but reshuffling the labels of the nodes. Doing so the number of clusters and the cluster sizes are maintained. In figure 5.15 an example of clustering with random labels, it is evident that all clusters have similar and homogeneous composition. Note that not every tissue has the same number of samples, so, for example, blood is more represented than other tissues.

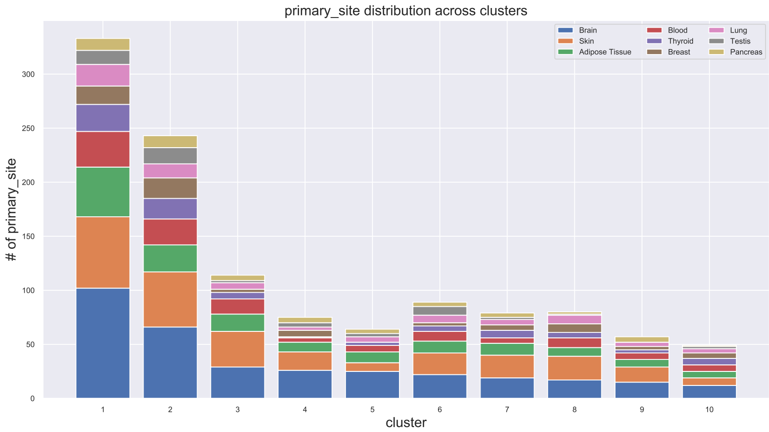

Figure 5.15: Example of visualization of clusters with reshuffled labels.

All the results described in the previous pictures are quite qualitative. To have a more objective and mathematical measure of the success of the algorithm it is possible to measure the fraction of the most representative label in each cluster k

$$max_{l \in labels}\left(\frac{n_{lk}}{n_k}\right)$$

with n_{lk} is the numbers of nodes labelled l in cluster k and n_k is the number of nodes in cluster k. This is represented in figure 5.16 for the level where the V-measure is maximized (best results are expected here). In figure 5.16 on the left is shown the most representative label fraction versus for each cluster, on the right the histograms of the same quantity. It is evident that models' clusters are very homogeneous with the majority of cluster with almost 100% of the same tissue. It is also clear that reshuffling the labels the result is very different and so the models behave better than expected. In figure 5.17 the same analysis is done for every level of the hierarchy. It is interesting to notice that at deeper levels (upper left in the figure) the random reshuffling and the real labels have the same behaviour. This is due to the fact that at this level clusters are very small and so it is easier to pick up nodes with the same level (in the extreme case of a cluster with size 1 it is always full with the same label). This shows that the deeper level it is not interesting, results are the same with random labels; moreover the reshuffling null model it is good to show up eventual biases due to small cluster sizes.

A similar analysis can be made considering not just the number of the cluster but the cluster size, this is shown in figure 5.18. It is interesting to notice that the shuffle null model and the real labels clusters are evidently different, so there must be some kind of signal. It is clear that the model is able to output big clusters full of the same

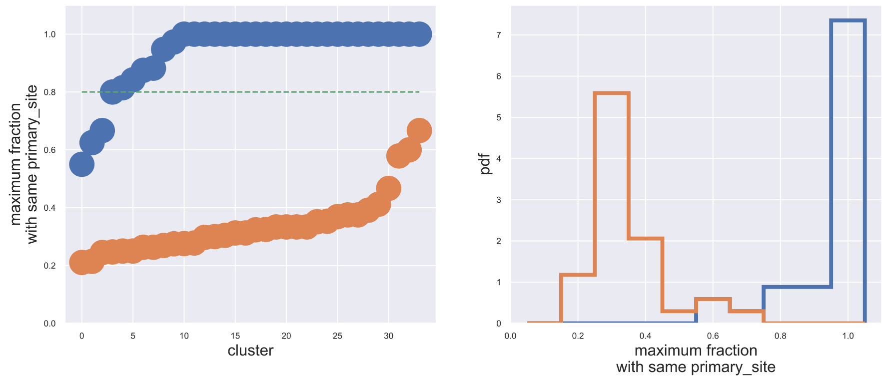

Figure 5.16: Most representative label versus cluster size.

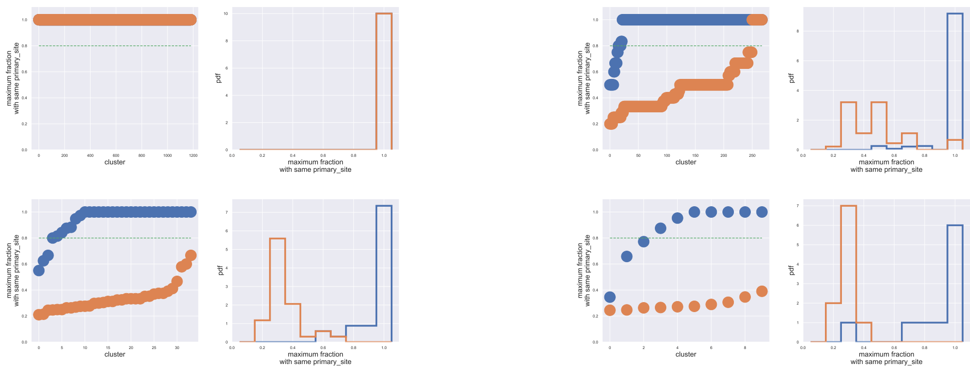

Figure 5.17: The fraction of the most representative label in all clusters for different levels of the hierarchy. From upper left the deeper layer than down right the upper one.

Figure 5.18: Fraction of most representative label versus cluster size.

label. In figure 5.19 the same analysis for all the levels of the hierarchy. It is interesting to see how going up in the hierarchy the two signals become different, as shown before the deeper layer (upper left in the image) is not different from null model and so it is not interesting.

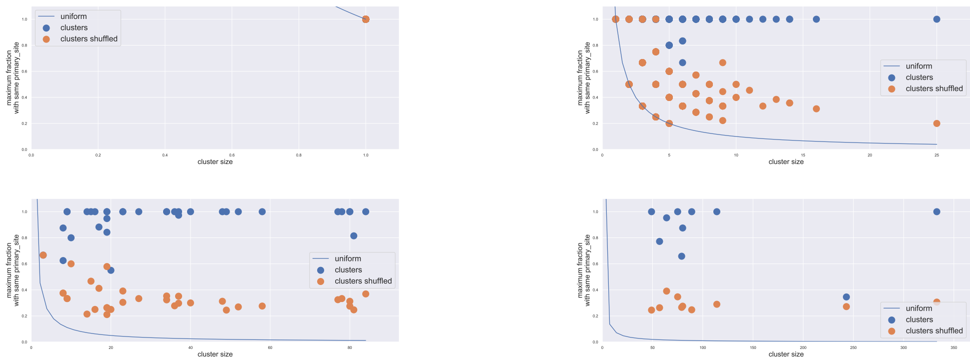

Figure 5.19: Fraction of most representative label versus cluster size across the hierarchy. From upper left the deeper layer than downright the upper one.

At this point to deepen investigate the structure of the clusters it can be interesting to study how many labels are present in each cluster. In fact, the fraction of most represented label defined above carries no information of what happens to the remaining labels. For example, if one cluster is composed of 80% by label **A** and 20% by label **B** and another cluster is composed 80% by label **A**, 10% by label **B** and 10% by label **C** they have both a fraction of maximum representative label 80% but the second in this example is more heterogeneous. Counting the number of different labels in each cluster can reveal this sort of effects. In figure 5.20 it is represented the number of different labels versus cluster size. It is evident that the reshuffling case is quite different from the real one, almost every cluster in the null model has got every label. It is interesting to notice that the model outputs even big cluster with one label. In figure 5.21 the same analysis for all the layer of the hierarchy. Even here the deeper level does not differ from the null model. Nevertheless in layers with higher V-measure score there is a strong signal that the reshuffling model is quite different from the model's output.

Having constructed the null model it is possible to estimate the V-measure score also for the null model. The results are reported in figure 5.22. Moreover remembering the V-measure or normalized mutual information defined in 5.4 it is possible to estimate a mixed score which considers the homogeneity of primary site and the completeness of secondary site, doing so the score goes up if going deeper in the hierarchy the model makes more cluster with the same tissue but separates sub tissues. It is not a big deal if one loses completeness regarding tissues (the model separates one big cluster full with the same label into two small ones) but gain information at the next magnification. This becomes clear if one looks at the big blood cluster that in the next level of the hierarchy is separated into two clusters of blood, one of whole blood and one of lymphocytes. The result is that this mixed score is the highest one.

Figure 5.20: The number of different labels in each cluster versus cluster size.

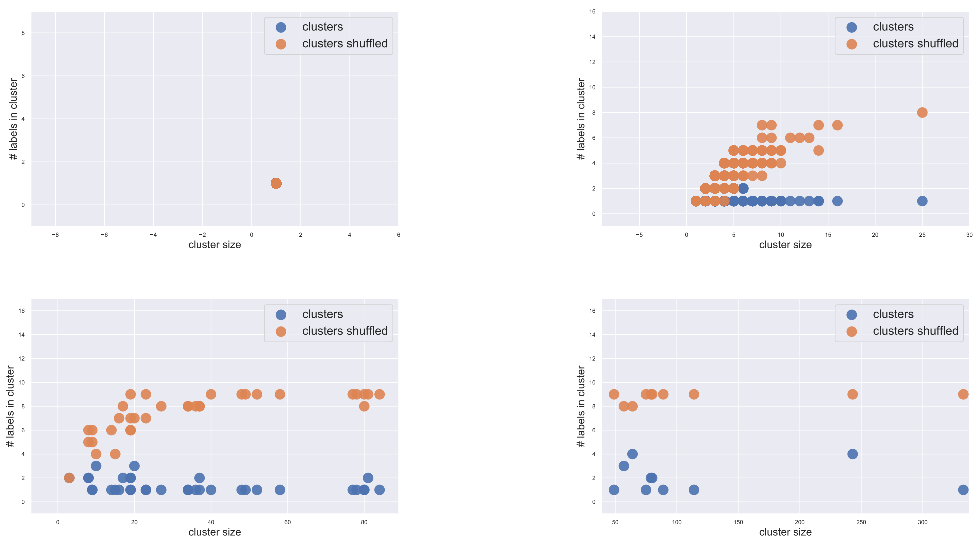

Figure 5.21: Number of different labels in each cluster versus cluster size. From upper left the deeper layer than downright the upper one.

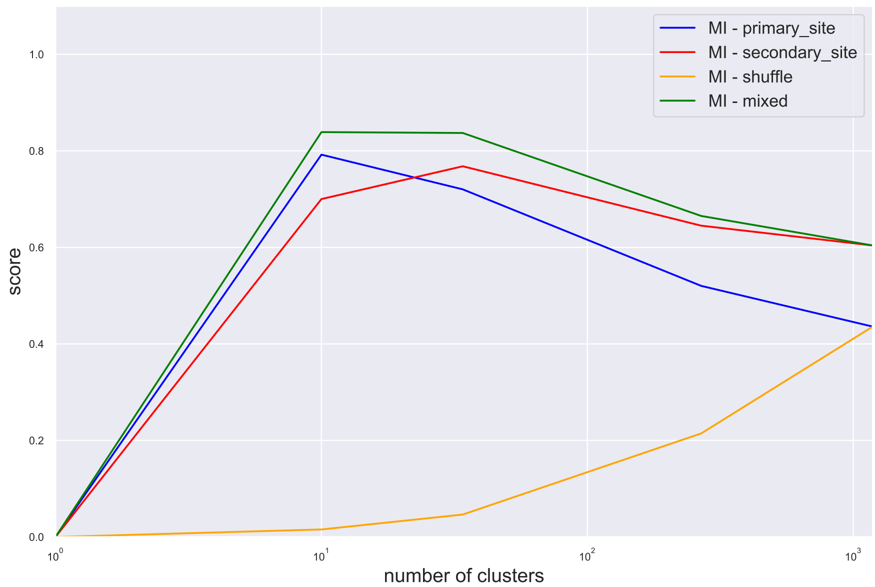

Figure 5.22: Scores across the hierarchy. The scored is compared with some random labels. In blue the score for the primary site labels, in red for the secondary site labels, in yellow the shuffled labels, in green the mixed score with primary homogeneity and secondary completeness.

5.3.3 Standard algorithms

At this point was verified that the model has got interesting output, it reaches high scores and has got a strong signal against the null model, at least at some levels of the hierarchy. It is now interesting to compare it with standard and well-known similar algorithms. First of all, a comparison is made with hierarchical clustering. This is done using the standard scipy [3] package, the metrics used was the euclidean one and the linkage method was set to Ward. This is quite fast, it needs a couple of minutes on a dual core, 8GB memory machine. In figure 5.23 the comparison between this scores, the hierarchical algorithm performs worse than hierarchical stochastic block model and as highly expected better than the random model.

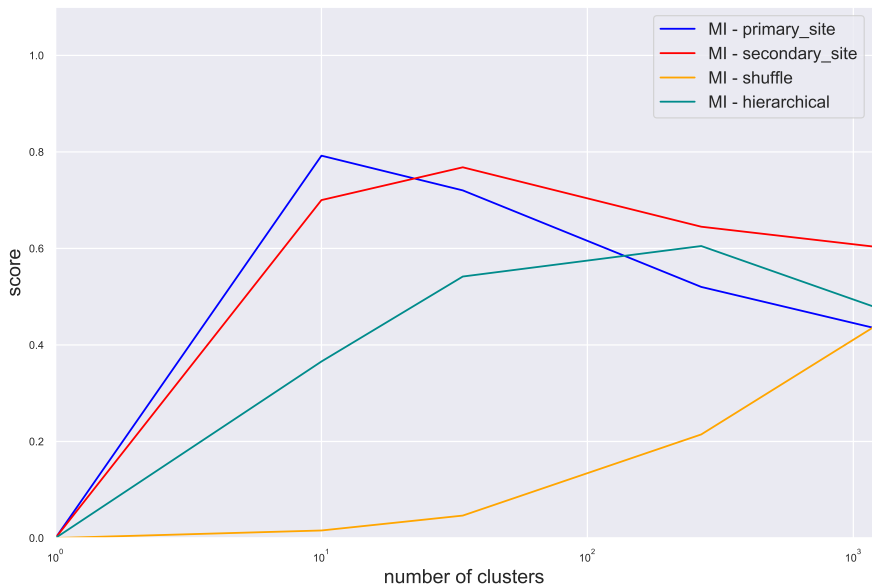

Figure 5.23: Scores across hierarchy. The scored is compared with some random labels

Another very used and well-studied algorithm is Latent Dirichlet Allocation briefly described in 5.1.2. Running LDA in standard scipy package is quite fast and is comparable with hierarchical clustering in terms of CPU time. Note that once LDA package extracts the topics, it is necessary to define some clusters, to do so a standard Agglomerative clustering approach was used, the distance was set to euclidean and the linkage to Ward. In figure 5.24 are reported the V-measure score for all the algorithms described until this point. What is clear is that the hierarchical Stochastic Block Model performs better than all the others, LDA gain a little worst score and hierarchical clustering is the worst of the three. As highly expected all models are quite different than random. The fact that hSBM and LDA have higher scores suggests that a topic model approach can be very useful in this kind of problems. Note that LDA and hierarchical cluster models were not fine tuned and default parameters were used. Maybe a fine tuning of this packages can lead to better and more satisfying results. This analysis,

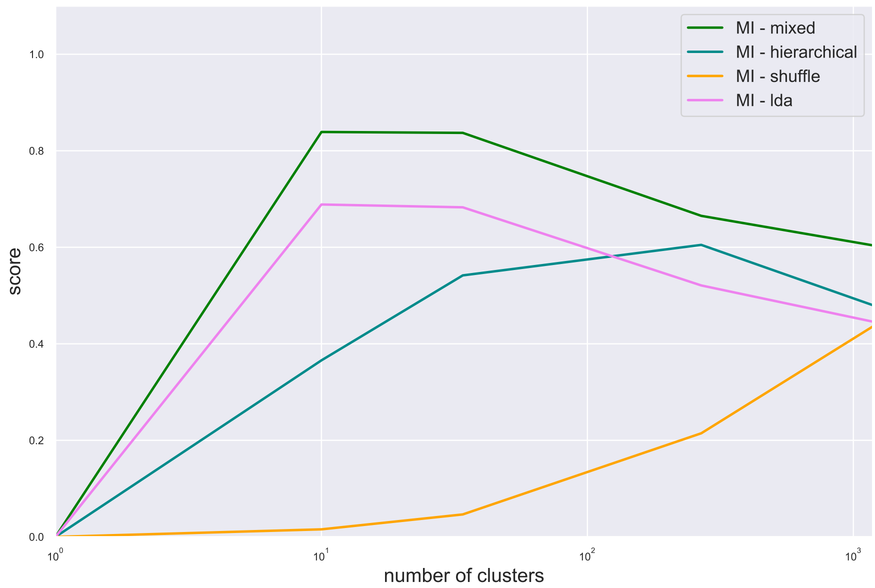

Figure 5.24: Scores across hierarchy. The scored is compared with some random labels

considering that the comparison was made with hierarchical Stochastic Block Model which is non-parametric and needs no setting, was done without any fine tuning and standard parameter were set. The fact reveals another good point of hSBM, it extracts not only better clusters, but also the parameters necessary to this kind of model.

5.3.4 Topics

The analysis up to this point considered only one of the two sides of the bipartite network, in fact nothing was told about the genes (words in topic models). Not less the model output some clusters of genes. From now on I'll refer to these clusters of genes as topics.

If one has got a set of genes in order to catch any important information and discover if there is any biological meaning behind it, it is possible to perform an enrichment test. Enrichment analysis checks whether an input set of genes significantly overlaps with annotated gene sets. In this work tests were made using Gene Set Enrichment Analysis [31] python tool [32], which performs a Fisher exact test (hypergeometric test), the Benjamini-Hochberg corrected P-values is reported. Genes' annotation terms were searched in the following sets:

- GO Molecular Function 2018
- GO Biological Process 2018
- GO Cellular Component 2018
- Human Phenotype Ontology

- Tissue Protein Expression from Human Proteome Map
- KEGG 2019 Human
- NCI-60 Cancer Cell Lines
- GTEx Tissue Sample Gene Expression Profiles up
- GTEx Tissue Sample Gene Expression Profiles down,

in particular the two latter contains annotation specific for GTEx dataset [33].

In tables 5.1, 5.2 and 5.3 are reported examples of enrichment test results for topics output by hSBM. On the results is put a P-value cut at 0.05 and terms are sorted by adjusted P-value. Test were made on the topics at the level of the hierarchy which

Term	Adjusted P-value	Gene set
pancreas male 60-69 years	1E-19	GTEx Tissue Sample Gene Expression Profiles up
pancreas female 40-49 years	3E-19	GTEx Tissue Sample Gene Expression Profiles up
pancreas male 40-49 years	5E-19	GTEx Tissue Sample Gene Expression Profiles up
pancreas male 30-39 years	1E-18	GTEx Tissue Sample Gene Expression Profiles up
pancreas female 20-29 years	1E-18	GTEx Tissue Sample Gene Expression Profiles up
pancreas male 50-59 years	1E-18	GTEx Tissue Sample Gene Expression Profiles up
pancreas female 30-39 years	1E-18	GTEx Tissue Sample Gene Expression Profiles up
pancreas male 50-59 years	2E-18	GTEx Tissue Sample Gene Expression Profiles up
pancreas male 40-49 years	2E-18	GTEx Tissue Sample Gene Expression Profiles up
pancreas male 30-39 years	2E-18	GTEx Tissue Sample Gene Expression Profiles up
pancreas male 50-59 years	2E-18	GTEx Tissue Sample Gene Expression Profiles up
pancreas female 20-29 years	2E-18	GTEx Tissue Sample Gene Expression Profiles up
pancreas male 40-49 years	3E-18	GTEx Tissue Sample Gene Expression Profiles up
pancreas female 50-59 years	4E-18	GTEx Tissue Sample Gene Expression Profiles up
pancreas male 50-59 years	4E-18	GTEx Tissue Sample Gene Expression Profiles up
pancreas male 50-59 years	4E-18	GTEx Tissue Sample Gene Expression Profiles up
pancreas female 60-69 years	5E-18	GTEx Tissue Sample Gene Expression Profiles up
pancreas female 50-59 years	5E-18	GTEx Tissue Sample Gene Expression Profiles up
pancreas male 50-59 years	5E-18	GTEx Tissue Sample Gene Expression Profiles up
pancreas male 30-39 years	6E-18	GTEx Tissue Sample Gene Expression Profiles up

Table 5.1: Enrichment test of a topic. It is clear the enrichment for pancreas related gene sets.

Term	Adjusted P-value	Gene set
brain female 40-49 years	6E-05	GTEx Tissue Sample Gene Expression Profiles up
brain male 50-59 years	6E-05	GTEx Tissue Sample Gene Expression Profiles up
brain female 60-69 years	6E-05	GTEx Tissue Sample Gene Expression Profiles up
brain female 60-69 years	6E-05	GTEx Tissue Sample Gene Expression Profiles up
brain female 60-69 years	6E-05	GTEx Tissue Sample Gene Expression Profiles up
brain female 40-49 years	6E-05	GTEx Tissue Sample Gene Expression Profiles up
brain female 40-49 years	6E-05	GTEx Tissue Sample Gene Expression Profiles up
brain female 60-69 years	6E-05	GTEx Tissue Sample Gene Expression Profiles up
brain male 60-69 years	6E-05	GTEx Tissue Sample Gene Expression Profiles up
brain male 50-59 years	6E-05	GTEx Tissue Sample Gene Expression Profiles up
brain male 50-59 years	6E-05	GTEx Tissue Sample Gene Expression Profiles up
brain male 60-69 years	7E-05	GTEx Tissue Sample Gene Expression Profiles up
brain male 50-59 years	7E-05	GTEx Tissue Sample Gene Expression Profiles up
brain male 20-29 years	7E-05	GTEx Tissue Sample Gene Expression Profiles up
brain female 60-69 years	8E-05	GTEx Tissue Sample Gene Expression Profiles up
brain female 60-69 years	8E-05	GTEx Tissue Sample Gene Expression Profiles up
brain female 60-69 years	1E-04	GTEx Tissue Sample Gene Expression Profiles up
brain female 60-69 years	1E-04	GTEx Tissue Sample Gene Expression Profiles up
brain female 60-69 years	1E-04	GTEx Tissue Sample Gene Expression Profiles up
brain male 60-69 years	1E-04	GTEx Tissue Sample Gene Expression Profiles up

Table 5.2: Enrichment test of a topic. It is clear the enrichment for brain related gene sets.

obtained the higher V-measure score on the sample side clustering. These results are

Term	Adjusted P-value	Gene set
blood male 50-59 years	3E-23	GTEx Tissue Sample Gene Expression Profiles up
blood male 50-59 years	3E-23	GTEx Tissue Sample Gene Expression Profiles up
blood male 40-49 years	3E-21	GTEx Tissue Sample Gene Expression Profiles up
blood male 60-69 years	9E-21	GTEx Tissue Sample Gene Expression Profiles up
blood male 40-49 years	3E-20	GTEx Tissue Sample Gene Expression Profiles up
blood female 60-69 years	4E-20	GTEx Tissue Sample Gene Expression Profiles up
blood male 60-69 years	4E-20	GTEx Tissue Sample Gene Expression Profiles up
blood female 50-59 years	5E-20	GTEx Tissue Sample Gene Expression Profiles up
blood female 50-59 years	1E-19	GTEx Tissue Sample Gene Expression Profiles up
blood male 60-69 years	1E-19	GTEx Tissue Sample Gene Expression Profiles up
blood male 60-69 years	1E-19	GTEx Tissue Sample Gene Expression Profiles up
blood female 60-69 years	1E-19	GTEx Tissue Sample Gene Expression Profiles up
blood male 60-69 years	2E-19	GTEx Tissue Sample Gene Expression Profiles up
blood male 50-59 years	2E-19	GTEx Tissue Sample Gene Expression Profiles up
blood female 40-49 years	2E-19	GTEx Tissue Sample Gene Expression Profiles up
blood female 40-49 years	2E-19	GTEx Tissue Sample Gene Expression Profiles up
blood female 60-69 years	2E-19	GTEx Tissue Sample Gene Expression Profiles up
blood male 30-39 years	3E-19	GTEx Tissue Sample Gene Expression Profiles up
blood female 50-59 years	5E-19	GTEx Tissue Sample Gene Expression Profiles up
blood female 60-69 years	5E-19	GTEx Tissue Sample Gene Expression Profiles up

Table 5.3: Enrichment test of a topic. It is clear the enrichment for blood related gene sets.

very interesting, these enrichment tests demonstrate that not only the sample side of the network is well clustered but only the topics have a non trivial meaning.

So also the topics are related to the tissues and somehow are tissue-specific. In the next examples the relation between the topics and the samples will be further investigated. In particular following what was done by [15] the importance of each topic inside each sample the $P(\text{topic}|\text{sample})$.

Separate healthy tissues is a good exercise and a good benchmark for models, but the real goals would be to be able to classify diseased samples. In fact it is not always easy to identify and classify cancer tissues. In particular being able to separate tumour sub-types would be the ideal pursuance of this work. So let's switch to the analysis of diseased samples.

5.3.5 Run on The Cancer Genomics Atlas

The exact same pipeline described so far ca be applied at other dataset. In this section the hSBM model is run on some samples from the TCGA. The principle is the same, but here samples comes from cancer tissues, so there must be more complexity and variability behind the data. Moreover being able to separate cancer samples is not always easy clinically and develop a method to do this can be highly interesting and useful for the scientific community [9].

First of all let's take a look at the V-measure scores. As shown in figure 5.25 the score is almost 0.7, which is good, but worse than the healthy GTEx scenario. In this dataset there is no a sub-tissue label as before, but a disease type cancer information is available. The disease type separation is not so good; the fact that there is no evident difference between Zipf's laws when separating data by disease type 3.17 means that all genes contributes to define this specif label so the pre-process filter is not a good option in this case. To gain better scores in this situation were samples are affected by the cancer complexity and heterogeneity is probably necessary to add more genes to the network.

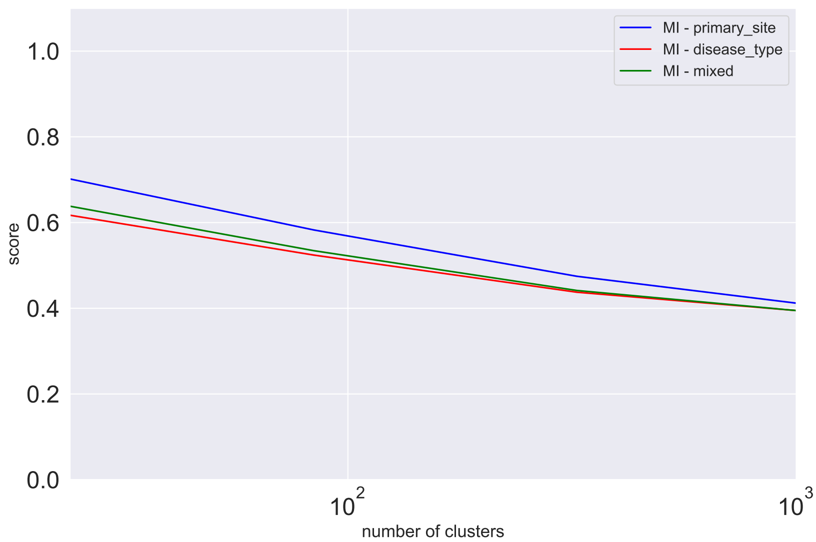

Figure 5.25: Score across the hierarchy for TCGA. In blue the primary site labels were considered, in red the disease types and in green the mix of the two.

Looking directly into the cluster composition the tissue separation is quite good and visually appreciable. In figure 5.26 clusters at the higher level of the hierarchy. Some tissues are well separated at this point, at the same time when possible samples are grouped by system, digestive system is the more evident. Going deeper in the hierarchy the tissue separation becomes visually appreciable and all the clusters are almost tissue-specific.

At this point when the model is demonstrated to work on healthy and diseased samples it can be interesting to study merged healthy and diseased labels and examine

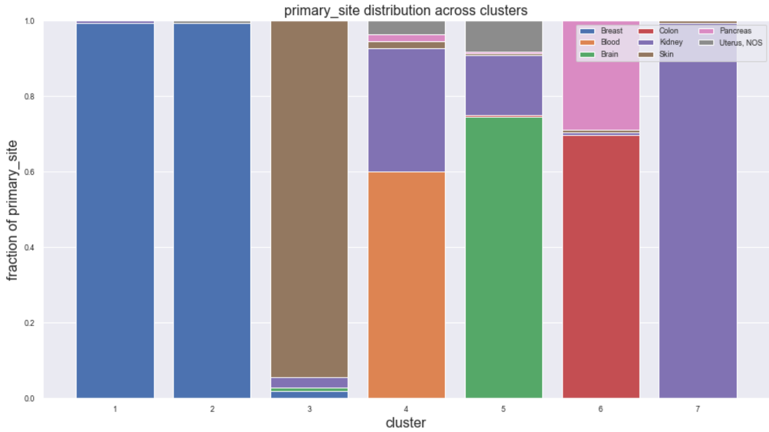

Figure 5.26: Clusters of diseased tissues at the higher level of the hierarchy. Breast is well separated, such as skin and brain. Cluster 6 contains digestive systems samples from pancreas and colon.

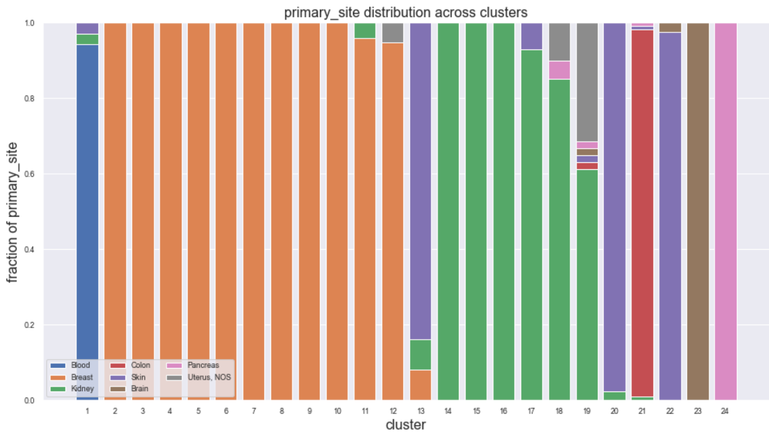

Figure 5.27: text

how the model behave when healthy and cancer samples are merged.

5.3.6 Healthy and diseased together

In th previous sections it was demonstrated that the model works on samples from different datasets and performs well on both healthy and diseased samples it can be interesting to see how the model behave when both kinds of data are presented to it. The goal of this part of work is to identify which genes or topics identify and distinguish tissues themselves and which drive cancer and are necessary to understand the differentiation between cancer types.

For this analysis were still analysed data from GTEx and TCGA, but from a particular dataset available from [17] were authors tried to unify the normalization process from different dataset and sources [16]. These are, in practice, a mixed bigger dataset; note that not every tissue is present in both GTEx and TCGA, so only common tissues are considered here. The first label considered at this point is the tissue primary site, forgetting about its status (healthy or diseased), the secondary label refers to the tissues but separates their status. For example, a healthy brain sample from GTEx and a cancer brain from TCGA share the *brain* primary site label but have different secondary site assignments.

Once the model is run, the first element to look at is the V-measure; in figure 5.28 the result for the primary site is quite satisfying: clusters are very homogeneous and V-measure's peak is near 0.8.

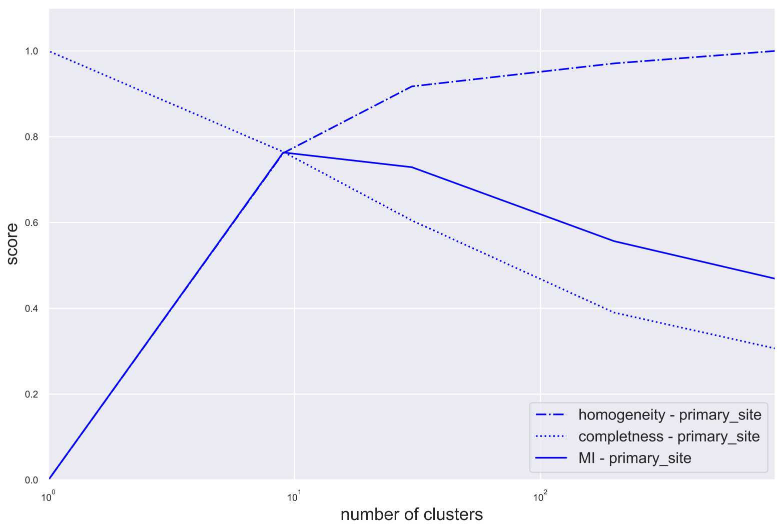

Figure 5.28: V-measure score for run with merged healthy and diseased samples. Homogeneity, completeness and mutual information are represented.

Estimating the score also for the secondary site, or rather for the tissues with the health state and for just the healthy/disease label lead to figure 5.29. This result is quite interesting, first of all even the secondary label is well classified and this happens at a deeper level respect to th one where tissues are separated; this means that firstly samples are separated by tissues then by their health state. This is very interesting because is an evidence that the model actually recognize tissues never mind where they come from, moreover the difference between datasets are not important here and so the normalization made by [16] brings no problems at this level. Moreover looking just at the health status label the score is quite low (below 0.2) so the model does not take over the difference between datasets. To conclude the score analysis a mixed score is

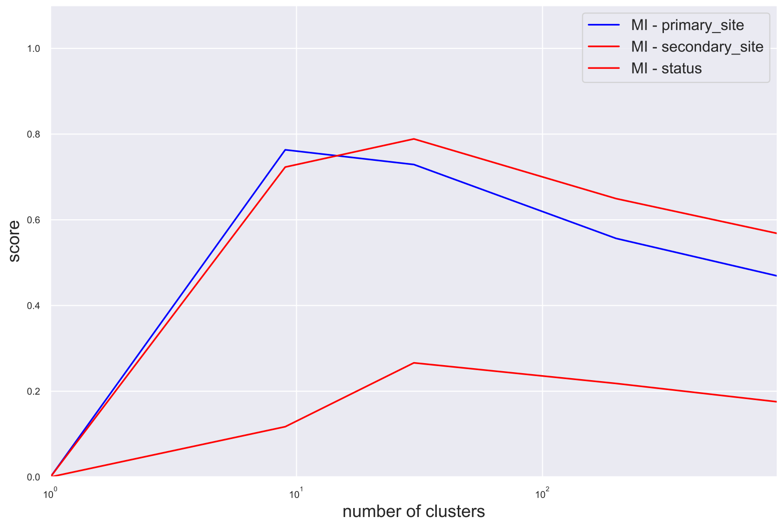

Figure 5.29: V-measure score for run with merged healthy and diseased samples. Primary site (brain, blood, pancreas..) labels are compared with secondary labels (healthy brain, brain cancer, healthy blood, blood cancer, healthy pancreas, pancreas cancer..). The health status label (healthy / diseased) is plotted.

considered (the homogeneity of primary site is considered with the completeness of secondary label) so that the score increase if going deeper in the hierarchy the separation of a homogeneous cluster brings to separation of the refined labels. In figure 5.30 this score is compared with the one obtained with LDA, hierarchical clustering and the null model. What happened here is that hierarchical Stochastic Block Model performs the best, LDA approach is good hierarchical clustering have a quite bad score and all are better than shuffling null model.

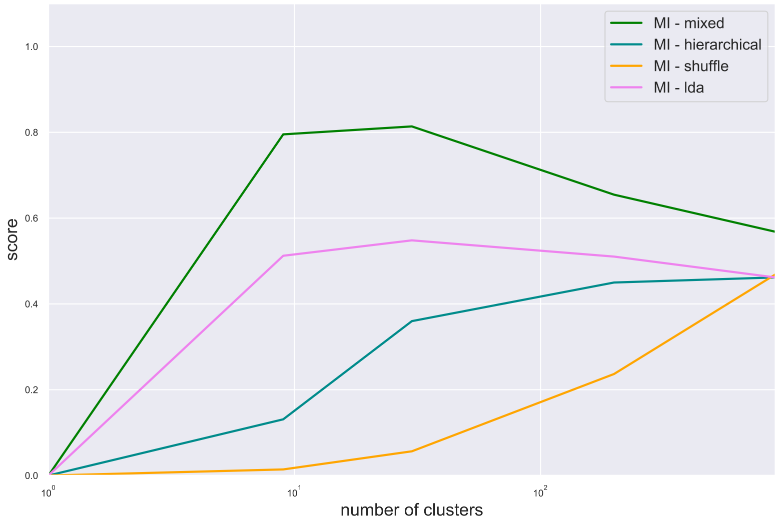

Figure 5.30: V-measure score for run with merged healthy and diseased samples. LDA, hierarchical clustering and null model for comparison.

Gene sets analysis is then performed. Considering the P-value of the term which P-value was the lowest, one P-value for each topic at the level of the hierarchy where the V-measure was maximized, it is possible to realize the $-Log_{10}(\mathrm{P-value})$ histogram. The tests are quite interesting, in fact there is an enrichment with a P-value lower than 0.05 in most cases so it is possible to assert that topics carry some interesting information more than expected by picking genes at random. In figure 5.32 are shown

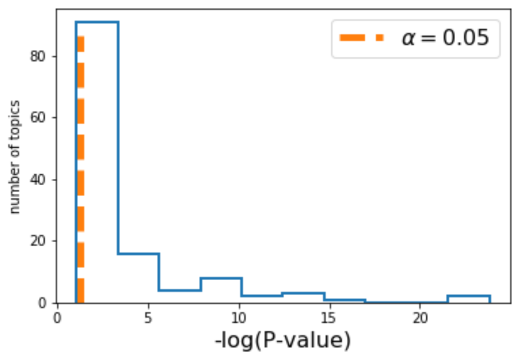

Figure 5.31: $-Log_{10}(\mathrm{P-value})$ of the term with the lowest P-value in each topic. In orange the classical 0.05 threshold.

the categories of the terms with lower P-values. This explains what aspect of the samples topic describes. The majority of terms found in topics comes from the GTEx annotation for tissue expression, many are from GO biological process, GO molecular function and some from Human phenotype ontology.

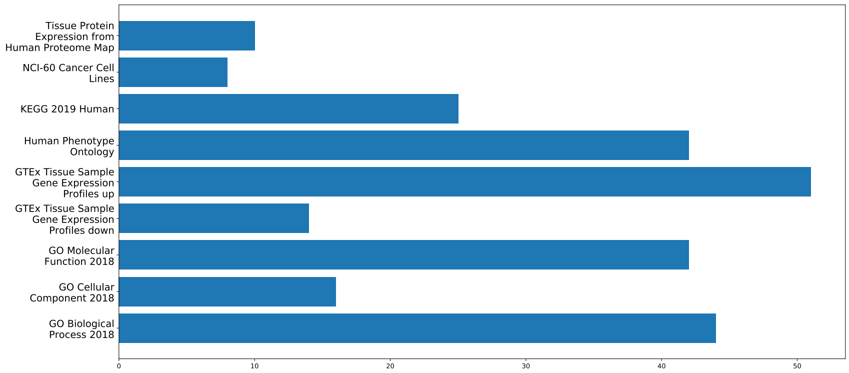

Figure 5.32: Categories of the terms with lower P-values in each topic.

Going forward in the analysis it is possible to perform enrichment test with other tools such as DAVID [34, 35]. Results are similar to the ones retrieved before. Tissues related terms are found also using this tool and this confirms the absence of tool or categories related biases. In figures 5.33, 5.34 and 5.35 the result from DAVID enrichment analysis. Finally it is interesting to notice that topics are quite small (order$\simeq$ 20 genes), so there are no biases that can appear doing enrichment tests on big sets.

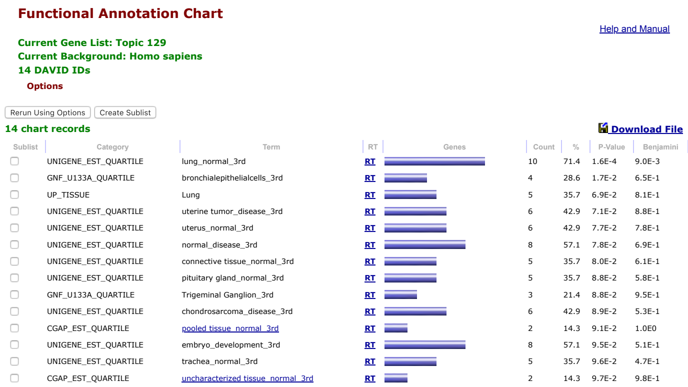

Functional Annotation Chart

Help and Manual

Current Gene List: Topic 129
Current Background: Homo sapiens
14 DAVID IDs
Options

Rerun Using Options | Create Sublist

14 chart records

Download File

Sublist	Category	Term	RT	Genes	Count	%	P-Value	Benjamini
	UNIGENE_EST_QUARTILE	lung_normal_3rd	RT		10	71.4	1.6E-4	9.0E-3
	GNF_U133A_QUARTILE	bronchialepithelialcells_3rd	RT		4	28.6	1.7E-2	6.5E-1
	UP_TISSUE	Lung	RT		5	35.7	6.9E-2	8.1E-1
	UNIGENE_EST_QUARTILE	uterine tumor_disease_3rd	RT		6	42.9	7.1E-2	8.8E-1
	UNIGENE_EST_QUARTILE	uterus_normal_3rd	RT		6	42.9	7.7E-2	7.8E-1
	UNIGENE_EST_QUARTILE	normal_disease_3rd	RT		8	57.1	7.8E-2	6.9E-1
	UNIGENE_EST_QUARTILE	connective tissue_normal_3rd	RT		5	35.7	8.0E-2	6.1E-1
	UNIGENE_EST_QUARTILE	pituitary gland_normal_3rd	RT		5	35.7	8.8E-2	5.8E-1
	GNF_U133A_QUARTILE	Trigeminal Ganglion_3rd	RT		3	21.4	8.8E-2	9.5E-1
	UNIGENE_EST_QUARTILE	chondrosarcoma_disease_3rd	RT		6	42.9	8.9E-2	5.3E-1
	CGAP_EST_QUARTILE	pooled tissue_normal_3rd	RT		2	14.3	9.1E-2	1.0E0
	UNIGENE_EST_QUARTILE	embryo_development_3rd	RT		8	57.1	9.5E-2	5.1E-1
	UNIGENE_EST_QUARTILE	trachea_normal_3rd	RT		5	35.7	9.6E-2	4.7E-1
	CGAP_EST_QUARTILE	uncharacterized tissue_normal_3rd	RT		2	14.3	9.7E-2	9.8E-1

Figure 5.33: Caption

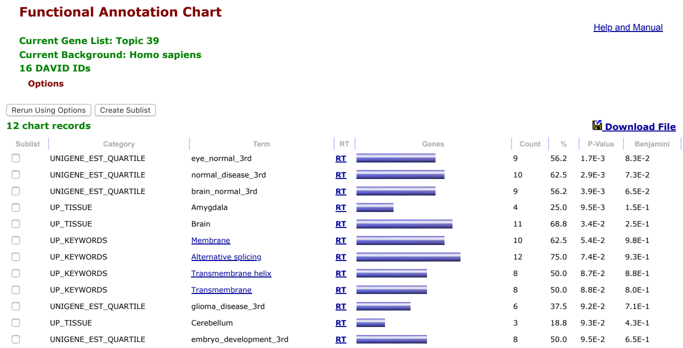

Functional Annotation Chart

Help and Manual

Current Gene List: Topic 39
Current Background: Homo sapiens
16 DAVID IDs
Options

Rerun Using Options | Create Sublist

12 chart records

Download File

Sublist	Category	Term	RT	Genes	Count	%	P-Value	Benjamini
	UNIGENE_EST_QUARTILE	eye_normal_3rd	RT		9	56.2	1.7E-3	8.3E-2
	UNIGENE_EST_QUARTILE	normal_disease_3rd	RT		10	62.5	2.9E-3	7.3E-2
	UNIGENE_EST_QUARTILE	brain_normal_3rd	RT		9	56.2	3.9E-3	6.5E-2
	UP_TISSUE	Amygdala	RT		4	25.0	9.5E-3	1.5E-1
	UP_TISSUE	Brain	RT		11	68.8	3.4E-2	2.5E-1
	UP_KEYWORDS	Membrane	RT		10	62.5	5.4E-2	9.8E-1
	UP_KEYWORDS	Alternative splicing	RT		12	75.0	7.4E-2	9.3E-1
	UP_KEYWORDS	Transmembrane helix	RT		8	50.0	8.7E-2	8.8E-1
	UP_KEYWORDS	Transmembrane	RT		8	50.0	8.8E-2	8.0E-1
	UNIGENE_EST_QUARTILE	glioma_disease_3rd	RT		6	37.5	9.2E-2	7.1E-1
	UP_TISSUE	Cerebellum	RT		3	18.8	9.3E-2	4.3E-1
	UNIGENE_EST_QUARTILE	embryo_development_3rd	RT		8	50.0	9.5E-2	6.5E-1

Figure 5.34: Caption

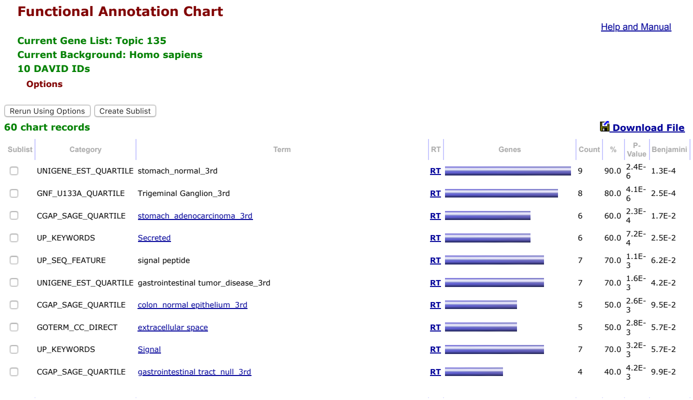

Functional Annotation Chart

Help and Manual

Current Gene List: Topic 135
Current Background: Homo sapiens
10 DAVID IDs
Options

Rerun Using Options | Create Sublist

60 chart records

Download File

Sublist	Category	Term	RT	Genes	Count	%	P-Value	Benjamini
	UNIGENE_EST_QUARTILE	stomach_normal_3rd	RT		9	90.0	2.4E-6	1.3E-4
	GNF_U133A_QUARTILE	Trigeminal Ganglion_3rd	RT		8	80.0	4.1E-6	2.5E-4
	CGAP_SAGE_QUARTILE	stomach_adenocarcinoma_3rd	RT		6	60.0	2.3E-4	1.7E-2
	UP_KEYWORDS	Secreted	RT		6	60.0	7.2E-4	2.5E-2
	UP_SEQ_FEATURE	signal peptide	RT		7	70.0	1.1E-3	6.2E-2
	UNIGENE_EST_QUARTILE	gastrointestinal tumor_disease_3rd	RT		7	70.0	1.6E-3	4.2E-2
	CGAP_SAGE_QUARTILE	colon_normal epithelium_3rd	RT		5	50.0	2.6E-3	9.5E-2
	GOTERM_CC_DIRECT	extracellular space	RT		5	50.0	2.8E-3	5.7E-2
	UP_KEYWORDS	Signal	RT		7	70.0	3.2E-3	5.7E-2
	CGAP_SAGE_QUARTILE	gastrointestinal tract_null_3rd	RT		4	40.0	4.2E-3	9.9E-2

Figure 5.35: Caption

The link between topics and samples has not been investigated so far. The probability distribution of each sample over topics $P(\text{topic}|\text{sample})$ can be estimated as

$$P(\text{topic}|\text{sample}) = \frac{\#\text{ of edges on sample from topic}}{\#\text{ of edges on sample}}$$

after the model is run. Moreover an average of all samples belonging to a topic can be estimated $P(\text{topic}|\text{tissue}) = \frac{1}{|tissue|}\sum_{sample \in tissue} P(\text{topic}|\text{sample})$.

In figure 5.36 it is plotted $P(\text{topic}|\text{tissue})$ for the first topics. What is clear is that in all samples there is a global trend that present no much differences between tissues, the topic expression differences between tissues are slightly appreciable at this point. This carries a profound and very informative message: under this new point of view in nature every tissue needs somehow the expression of all the genes (there is a global trend) and small differences between genes' expression are fine tuned to obtain different tissues. In other words it is possible to describe human tissues assuming that all genes are important and that is the fine structure of their interactions which realizes the complexity observed. In the case of diseased samples this suggest that it should be possible to discover a cancer type not looking at a few marker genes but looking at the whole expression profile of all genes. In order to better understand these differences between topic expression in different tissues some kind of normalization inside each topic is needed. Here it was chosen to study inside each topic which tissues

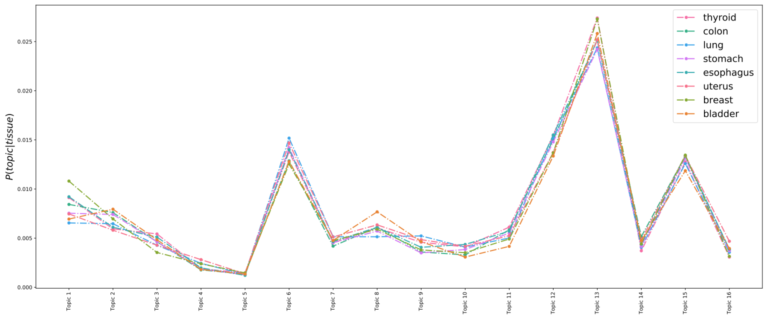

Figure 5.36: $P(\text{topic}|\text{tissue})$ for some topic colored by tissue. It is clear a global trend and in some topics there are little differences between tissues.

are most differently expressed than average. To do so from each $P(\text{topic}|\text{tissue})$was subtracted the average topic expression $\text{mean}_{\text{tissue}}(\text{topic}) = \langle P(\text{topic}|\text{tissue})\rangle_{tissue}$ and the result was divided by the standard deviation $\sigma_{\text{tissue}}(\text{topic})$. In figure 5.37 some most characteristic topics are reported. This analysis reveals that tissue have a different behaviour than average in different topics, different tissues are distant from the average in different topics. Moreover, the healthy and the disease sample from the two different sources seems to have a similar behaviour, in fact if a healthy tissue is far from the average in a topic, the diseased counterpart is also distant from the average as evident in the topics reported in the figure.

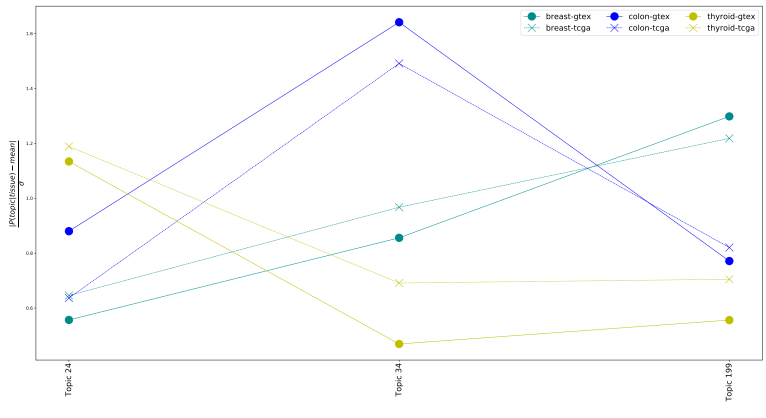

Figure 5.37: $\frac{\left|P(topic|tissue) - \langle P(\text{topic}|\text{tissue})\rangle_{tissue}\right|}{\sigma_{\text{tissue}}(\text{topic})}$ or the distance of each tissue from the average tissue expression in each topic. Some interesting topics are reported.

The study of the relation between topics and samples conclude the topic modelling analysis. In the next section all results achieved will be summarized.

5.4 Results

The analysis using topic modelling leads to many interesting results.

The first result achieved is the development of a model that is able to reproduce the distinction between different tissues from RNA-sequencing datasets. This is evident looking at the cluster composition. Moreover, if one defines more objective metrics based on the entropy the score is quite high, this encouraged further analysis. In particular, in many cases, the model not only reproduces the main tissue classification but was demonstrated that at different layers of the hierarchy even the sub-tissue labels are distinguished. The mutual information score confirms this model's behaviour: tissues are separated at a higher level of the hierarchy and in the deeper layers the sub-tissues are distinguished.

A null model realized shuffling the labels confirms that the results achieved are non-trivial. Studying some quantities such as the fraction of cluster with the same label and comparing these with the null models' ones it is possible to affirm that clusters are more homogeneous than expected.

The output of the model presented in this work (hSBM) was compared with more standard approaches such as Latent Dirichlet Allocation and hierarchical clustering. hSBM outputs better results with respect to standard approaches, moreover, it gains higher scores. An interesting fact is that topic modelling (both LDA and hSBM) is better than standard algorithms. This confirms the good quality of a topic model approach and, inside topic models, hSBM seems better than LDA. All algorithms are distant from the null model as highly expected.

It was also demonstrated that not only clustering of the sample was satisfying but even the genes' classification is interesting. If one looks at the block of genes, the so-called topics, enrichment tests confirm that topics represent interesting group of genes. In particular, some dataset-specific labels were found in GTEx analysis.

In the end, the relationship between samples and topics reveals interesting facts. The distribution of the topic abundance across samples reveals that it is possible to describe the tissue differentiation as a complex mechanism of relationships between genes' expression. This isn't possible using a LDA approach where genes can be either present or absent in a sample. Biologically this means that all genes are necessary everywhere and a fine-tuning of their expression differentiate by tissue.

The sample clustering, topic analysis and the relationship between samples and topics were made on three different datasets. GTEx containing just healthy samples, TCGA containing cancer samples and [17] which merged the two. Analysing the dataset with both healthy and diseased samples the differentiation between tissues is still evident and going deeper in the hierarchy the separation involves also the healthy or diseased status. The tissue separation in the firsts layer confirms that what the algorithm does is separating tissues and there is no, evident, bias between datasets.

Each of these cases reveals interesting facts. Being able to reproduce GTEx labels is a good benchmark of the quality of the algorithm; to accurately reproduce TCGA labels is the real challenge that can improve scientific community knowledge and here was partially achieved. Analysing both at the same time helps in understanding which genes are somehow involved in cancer development.

Chapter 6

Conclusions

Finally this work demonstrates that RNA-Sequencing datasets can be analyses from a component systems point of view. This kind of data shows typical trends famous, for example, in linguistics, moreover some interesting biological signatures were found. RNA-Seq dataset have a great core of protein coding genes that express everywhere, this is evident looking at Us, Heaps' law. The presence of a power law distribution in the ranked abundances, the so called Zipf's law is observed and characterize the distribution of genes expression data.

In the first part of this work a dataset (GTEx) containing samples from healthy tissues was analysed. One of the most interesting evidences was the presence of many different Zipf's law if one considers each tissue independently. Very similar results were obtained considering TCGA, a dataset containing thousands of samples of cancer tissues.

The power law distribution encouraged to explore the possibility of using a topic model approach to reveal the hidden structure of these datasets. This approach is useful both to find clusters of samples that share some properties and to find the relation between genes and samples.

Many goals were achieved during these analysis. First of all it was developed a pipeline that begins with creating a network with useful genes and samples, this network is than processed with hierarchic stochastic block model topic model algorithm and then analysed.

In conclusion topic model reveal itself as a useful approach to this kind of data.

Verified that benchmark give good results the next goal would be to

future: Loredana, Jacopo, topic on sampling, Jonathan

Appendix A

Hierarchical stochastic block model

The algorithm is called hierarchic Stochastic Block Model.

The first step of hierarchical stochastic block model, as discussed in [36], is to create a bipartite network G with two kind of nodes: **words** and **documents**. Every time a word w is present in a document d an edge e_{wd} is created. If a word count in the entire corpus is under a certain threshold, that word is ignored. The aim is to find a partition $b \in \{b_i\}$ with $B = |\{b_i\}|$ blocks.

These kind of models are called *generative models*: given the data the model should generate a network G with probability $P(G|\theta, b)$, where b is the partition and θ any additional parameter of the model.

Using well-known Bayes theorem one could estimate the probability that an observed network is generated by partition b

$$P(b, \theta|G) = \frac{P(G|b, \theta)\overbrace{P(b, \theta)}^{prior}}{\underbrace{P(G)}_{\sum_\theta P(G|\theta,b)P(\theta,b)}} \tag{A.1}$$

defining the amount of information needed to describe the data as the description length

$$\Sigma = -lnP(G|b, \theta) - lnP(b, \theta) \tag{A.2}$$

the A.1 can be written as $\frac{e^{-\Sigma}}{P(G)}$, so maximising that is equivalent to minimise the description length A.2. The probability of obtaining a Graph from a set of parameters is $P(G|b, \theta) = \frac{1}{\Omega(A, \{n_r\})}$, where $\Omega(A, \{n_r\})$ is the number of graph that is possible to generate with audience matrix A and n_r the counts of block partition $\{b_i\}$

In case of a weighted network the likelihood becomes $P(G, x|b, \theta)$, where x are the weights.

Algorithm First of all a $B \times B$ matrix is created. The entry e_{rs} of this matrix represents the number of links between nodes of group r and nodes of group s, with $r, s \in \{b_i\}$. At the beginning B groups are formed at random and the initial B is a hyper-parameter of the model.

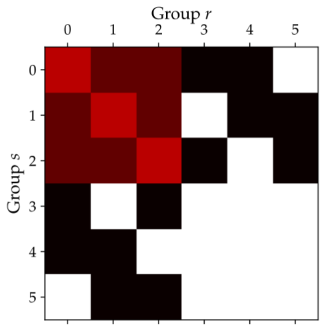

Figure A.1: Example of a edge's matrix from [8]

It is useful to define a traditional entropy:

$$S_t = \frac{1}{2}\Sigma_{r,s} n_r n_s H\left(\frac{e_{rs}}{n_r n_s}\right) \tag{A.3}$$

where n_r is the number of nodes in groups r, e_{rs} is the number of edges between nodes of group r and nodes of group s, and $H(x) = -xln(x) - (1-x)ln(1-x)$. This entropy is equivalent to the micro-canonical entropy of a system with $\Omega(A, \{n_r\})$ accessible states $S_t = Ln\Omega$.

The algorithm uses a Markov Chain Monte Carlo to minimise this entropy. At each step a node changes block and the new configuration is accepted if S is decreased.

Note that A.3 can be corrected taking care of degree distribution obtaining corrected entropy S_c

$$S_c = -\Sigma_{r,s}\frac{e_{rs}}{2} - \Sigma_k N_k ln(k!) - \frac{1}{2}\Sigma_{r,s} e_{rs} ln\left(\frac{e_{rs}}{e_r e_s}\right) \tag{A.4}$$

How to change group of a node? At each step according to [36] node i can change group from r to s with a probability

$$P(r \to s|t) = \frac{e_{ts} + \epsilon}{e_t + \epsilon B} \tag{A.5}$$

where j is a random neighbour of i: $j \in N_i$, $t \in \{b_j\}$ its block as defined in [36]. ϵ is a parameter that according to [29] has no significant impact in the algorithm, provided it is sufficiently small.

A.5 can be rewritten as

$$P(r \to s|t) = (1 - R_t)\frac{e_{ts}}{e_t} + \frac{R_t}{B}$$

defining $R_t = \frac{\epsilon B}{e_t + \epsilon B}$

This is done in four steps for each node i:

- a node j is chosen from i's neighbours, the group of j is called t
- a random group s is selected

- move of node i to group s is accepted with probability R_t
- if s is not accepted, a random edge e is chosen from group t and node i is assigned to the endpoint of e which is not in t

This steps mime probability A.5; note that for $\epsilon \to \infty$ this gives a uniform probability.

To enchant the probability to go into a minimum, a bounce of these moves is made, only the set of moves with the minimum S is accepted.

How many blocks B? Note that the number of blocks B is a free parameter and must be inferred as described in [29]. This implies a slight modification of the algorithm such that it became possible to admit that a new group is created. When a group s is chosen, the algorithm can now accept a **new group** and A.5 became

$$P(r \to s) = \Sigma_t P(t|i) \frac{e_{ts} + \epsilon}{e_t + \epsilon(B+1)} \tag{A.6}$$

being $P(t|i) = \Sigma_j \frac{A_{ij}\delta(b_j,t)}{k_i}$ the fraction of neighbours of i belonging to group t, e_t the number of edges in group t, k_i the degree, and b_j groups.

Using this modification it is now possible to add new groups and B is no longer a parameter.

How to find hierarchic layers? After the algorithm is run, one may would to add a new hierarchic level, this is done considering the B groups as nodes and repeating the process. As done before a matrix of edges like A.1 is created, where edges are considered between groups of the previous layer.

The posterior probability became

$$P(\{b_l\}|A) = \frac{P(A|\{b_l\})P(\{b_l\})}{P(A)} = \prod_{l}^{L} P(b_l|e_l, b_{l-1}) \tag{A.7}$$

where $l = 0 \dots L$ is the layer, A the audience matrix, b_i blocks. Note that $e_0 = A$ and $B_L = 1$. Maximising A.7 gives the correct number of layers.

Adding a layer is done in 3 steps described in [37]:

Resize find $B_l \in [B_{l-1}, B_{l+1}]$ by bisection

Insert a layer l

Delete l and linking nodes from layer $l-1$ directly to groups of layer $l+1$

One marks initially all levels as not done and starts at the top level $l = L$ [37]. For the current level l, if it is marked done it is skipped and one moves to the level $l-1$. Otherwise, all three moves are attempted. If any of the moves succeeds in decreasing the description length Σ A.2, one marks the levels $l-1$ and $l+1$ (if they exist) as not done, the level l as done, and one proceeds (if possible) to the upper level $l+1$, and repeats the procedure. If no improvement is possible, the level l is marked as done and one proceeds to the lower level $l-1$. If the lowest level $l = 0$ is reached and cannot be improved, the algorithm ends.

Overlapping partitions As described in [38] one of the advantages of this approach is that it is possible to let a node belonging to multiple groups. In this case b_i becomes $\vec{b_i}$, with component $b_{ir} = 1$ if node i is in group r, 0 otherwise. The number of 1s in vector $\vec{b_i}$ is called $d_i = |\vec{b_i}|$.

The probability of having a graph G being generated from an audience matrix A and a partition $\{\vec{b_i}\}$ is

$$P(G|A, \{\vec{b_i}\}) = \frac{1}{\Omega}$$

if Ω is the number of possible graphs. Entropy A.3 is $S_t = Ln\Omega$. This corresponds to an augmented graph generated via a non overlapping block model with $N' = \Sigma_r n_r > N$ nodes and the same audience matrix A.

First of all, it is necessary to sample the distribution of mixture sizes $P(\{n_d\})$ where n_d is the number of nodes which mixture has got size d, $n_d \in [0, N]$ and $d \in [0, D]$ (typically $D = B$ and in the non-overlapping case $D = 1$), this is done by sampling uniformly from

$$P(\{n_d\}|B) = \left(\!\!\binom{D}{N}\!\!\right)^{-1}$$

which is probability of having n nodes whose mixture has size d. $\left(\!\binom{B}{N}\!\right)$ is the number of histograms with area N and B distinguishable bins. $B - 1$ can be used instead of B to avoid node with no group, in this case $d \in [1, B]$.

Given the mixture sizes, the distribution of node membership is sampled from

$$P(\{d_i\}|\{n_d\}) = \frac{\prod_d n_d!}{N!}$$

.

At this point for each set of nodes with $d_i = d$ it is necessary to sample $n_{\vec{b}}$; the number of nodes with a particular mixture $\vec{b}$. It is sampled from

$$P(\{n_{\vec{b}}\}_d|n_d) = \left(\!\!\binom{\binom{D}{d}}{n_d}\!\!\right)^{-1}, \tag{A.8}$$

next all mixtures $\vec{b_i}$ of size d must be sampled, they are given by

$$P(\{\vec{b_i}\}_d|\{n_{\vec{b}}\}_d) = \frac{\prod_{|\vec{b_i}|=d} n_b!}{n_d!} \tag{A.9}$$

the global posterior as defined in [38] is

$$P(\{\vec{b_i}\}|B) = \left[\prod_{d=1}^{B} P(\{\vec{b_i}\}_d|\{n_{\vec{b}}\}_d)P(\{n_{\vec{b}}\}_d|n_d)\right] P(d_i|n_d)P(n_d|B) \tag{A.10}$$

At this time it is necessary to obtain the distribution of the edges between mixtures. Defined $e_r = \Sigma_s e_{rs}$ the number of half-edges labelled r, $m_r = \Sigma_{\vec{b}} b_r$ the number of mixtures containing group r the algorithm samples the probability distribution of the edges count

$$P(\{e_{\vec{b}}\}|\{\vec{b_i}\}, A) = \prod_r \left(\!\!\binom{m_r}{e_r}\!\!\right)^{-1}$$

and the labeled degree sequence $\{\vec{k}_i\}$ from

$$P(\{\vec{k}_i\}_{\vec{b}}|\{e_{\vec{b}}\},\{\vec{b}_i\}) = \frac{\prod_k n_k^{\vec{b}}!}{n_{\vec{b}}!}$$

Word documents separation Following what is done in [27], the probability of a group $P(b_l)$ at a certain level l is intended as the disjoint probability of group of words and group of documents.

$$P(b_l) = P_w(b_l^w)P_d(b_l^d) \tag{A.11}$$

Doing this let words and documents be separated by construction. Considering the process described above if two nodes are not connected at the beginning it is impossible that they end up in the same block. It is easily verified in [36] that this property is preserved and fully reflected in the final block structure.

Appendix B

Homogeneity, completeness and V-measure

Using algorithms that are unsupervised, but with a ground truth available it is useful to define some metrics.

The homogeneity

$$h = 1 - \frac{H(C|K)}{H(C)} \tag{B.1}$$

defining the entropy

$$H(C|K) = \sum_{c \in \text{modellabels}, k \in \text{clusters}} \frac{n_{ck}}{N} Log \left(\frac{n_{ck}}{n_k} \right) \tag{B.2}$$

where n_{ck} is the number of nodes of type c in cluster k, N the number of nodes and n_k the number of nodes in cluster k. It is evident that if all nodes inside cluster k are of the same type c $n_{ck} = n_k$, $H(C|K) = 0$ and $h = 1$, it is actually a full homogeneous situation. The completeness:

$$c = 1 - \frac{H(K|C)}{H(K)}, \tag{B.3}$$

$H(K|C)$ is defined in the same way as $H(C|K)$. Completeness measures if all nodes of the same type are in the same cluster. Ideally one wants a model which output is both homogeneous and complete. So it is possible to define the V-measure [30], which is the harmonic average of the two:

$$2\frac{hc}{h+c}. \tag{B.4}$$

The product hc is equal to

$$\frac{(H(C) - H(C|K))(H(K) - H(K|C))}{H(K)H(C)}, \tag{B.5}$$

the sum $h + c$ is

$$\frac{H(K)(H(C) - H(C|K)) + H(C)(H(K) - H(K|C))}{H(K)H(C)}. \tag{B.6}$$

Expressing the conditional entropy

$$H(K|C) = \sum_{kc} P(k,c)Log(P(k|c)) = \sum_{kc} P(k,c)Log\left(\frac{P(k,c)}{P(c)}\right) = H(K,C) - H(C)$$

in terms of the conjunct entropy $H(K,C)$ which is symmetric by exchanges of C and K

$$H(K,C) = H(K|C) + H(C) = H(C|K) + H(K) = H(C,K)$$

it is easy to verify that

$$H(C) - H(C|K) = H(K) - H(K|C)$$

so

$$hc = \frac{(H(C) - H(C|K))^2}{H(K)H(C)}$$

and

$$h + c = \frac{(H(C) - H(C|K))(H(K) + H(C))}{H(K)H(C)}.$$

The harmonic average $2\frac{hc}{h+c}$ gives

$$\mathrm{V-measure} = 2\frac{H(C) - H(C|K)}{H(K) + H(C)} = 2\frac{H(C) + H(K) - H(K,C)}{H(K) + H(C)} = 2\frac{MI(C,K)}{H(K) + H(C)}$$

which is actually the mutual information between $P(C)$ and $P(K)$ normalized to 1 by the term $H(C) + H(K)$. In fact if $P(C) = P(K)$ $H(K,C) = H(K) = H(C)$ and the measure is 1, if $P(C)$ and $P(K)$ are completely independent $H(K,C) = H(K) + H(C)$ and the measure is 0.

List of Figures

List of Tables

Bibliography

[1] J. Siek, A. Lumsdaine, and L.-Q. Lee, *The boost graph library: user guide and reference manual*. Addison-Wesley, 2002.

[2] W. McKinney *et al.*, "Data structures for statistical computing in python," in *Proceedings of the 9th Python in Science Conference*, vol. 445, pp. 51–56, Austin, TX, 2010.

[3] E. Jones, T. Oliphant, and P. Peterson, "{SciPy}: Open source scientific tools for {Python}," *[Online; accessed 2019-07-12]*, 2014.

[4] T. E. Oliphant, *A guide to NumPy*, vol. 1. Trelgol Publishing USA, 2006.

[5] J. D. Hunter, "Matplotlib: A 2d graphics environment," *Computing in science & engineering*, vol. 9, no. 3, pp. 90–95, 2007.

[6] M. A. et al., "TensorFlow: Large-scale machine learning on heterogeneous systems," 2015. Software available from tensorflow.org.

[7] Z. et al., "Apache spark: A unified engine for big data processing," *Commun. ACM*, vol. 59, pp. 56–65, Oct. 2016.

[8] T. P. Peixoto, "The graph-tool python library," *figshare*, 2014.

[9] TCGA Research Network, "Cell-of-Origin Patterns Dominate the Molecular Classification of 10,000 Tumors from 33 Types of Cancer," *Cell*, vol. 173, no. 2, pp. 291–304.e6, 2018.

[10] W. Zhou, S. Yao, L. Liu, L. Tang, and W. Dong, "An overview of topic modeling and its current applications in bioinformatics," *Springerplus*, 2016.

[11] A. Lancichinetti, M. Irmak Sirer, J. X. Wang, D. Acuna, K. Körding, and L. A. Amaral, "High-reproducibility and high-accuracy method for automated topic classification," *Phys. Rev. X*, 2015.

[12] A. Martini, A. Cardillo, and P. D. L. Rios, "Entropic selection of concepts unveils hidden topics in documents corpora," *arXiv*, 2017.

[13] Z. Wang, M. Gerstein, and M. Snyder, "Rna-seq: a revolutionary tool for transcriptomics," *Nature reviews genetics*, vol. 10, no. 1, p. 57, 2009.

[14] R. L. Grossman, A. P. Heath, V. Ferretti, H. E. Varmus, D. R. Lowy, W. A. Kibbe, and L. M. Staudt, "Toward a shared vision for cancer genomic data," *New England Journal of Medicine*, vol. 375, no. 12, pp. 1109–1112, 2016.

[15] K. K. Dey, C. J. Hsiao, and M. Stephens, "Visualizing the structure of rna-seq expression data using grade of membership models," *PLoS genetics*, vol. 13, no. 3, p. e1006599, 2017.

[16] D. Betel, A. Ochoa, C. Zhang, A. V. Penson, L. Zhang, N. Schultz, C. A. Iacobuzio-Donahue, B. E. Gross, Q. Wang, J. Armenia, J. Gao, E. Reznik, T. Minet, and B. S. Taylor, "Unifying cancer and normal RNA sequencing data from different sources," *Sci. Data*, 2018.

[17] Q. Wang, J. Gao, and N. Schultz, "Unified RNA-seq datasets in human cancers and normal tissues - normalized data," *figshare*, 2017.

[18] L. J. Carithers, K. Ardlie, *et al.*, "A novel approach to high-quality postmortem tissue procurement: the gtex project," *Biopreservation and biobanking*, vol. 13, no. 5, pp. 311–319, 2015.

[19] A. Mazzolini, A. Colliva, M. Caselle, and M. Osella, "Heaps' law, statistics of shared components, and temporal patterns from a sample-space-reducing process," *Physical Review E*, vol. 98, no. 5, p. 052139, 2018.

[20] A. Mazzolini, J. Grilli, E. De Lazzari, M. Osella, M. C. Lagomarsino, and M. Gherardi, "Zipf and Heaps laws from dependency structures in component systems," *Phys. Rev. E*, vol. 98, p. 012315, jul 2018.

[21] E. G. Altmann and M. Gerlach, "Statistical laws in linguistics," in *Creativity and Universality in Language*, pp. 7–26, Springer, 2016.

[22] A. Mazzolini, M. Gherardi, M. Caselle, M. Cosentino Lagomarsino, and M. Osella, "Statistics of Shared Components in Complex Component Systems," *Phys. Rev. X*, vol. 8, p. 021023, apr 2018.

[23] H. S. Heaps, *Information Retrieval: Computational and Theoretical Aspects*. Orlando, FL, USA: Academic Press, Inc., 1978.

[24] M. Melé, F. Pedro, R. Ferran, D. S. DeLuca, M. Jean, S. Micheal, K. Ardlie, and G. Roderic, "The human transcriptome across tissues and individuals," *Science (80-.).*, vol. 348, no. 6235, pp. 660–665, 2014.

[25] Z. Eisler, I. Bartos, and J. Kertész, "Fluctuation scaling in complex systems: Taylor's law and beyond1," *Adv. Phys.*, vol. 57, pp. 89–142, jan 2008.

[26] S. Islam, A. Zeisel, S. Joost, G. La Manno, P. Zajac, M. Kasper, P. Lönnerberg, and S. Linnarsson, "Quantitative single-cell RNA-seq with unique molecular identifiers," *Nat. Methods*, vol. 11, p. 163, dec 2013.

[27] M. Gerlach, T. P. Peixoto, and E. G. Altmann, “A network approach to topic models,” *Science advances*, vol. 4, no. 7, p. eaaq1360, 2018.

[28] P. W. Holland, K. Blackmond, and S. Leinhardt, “STOCHASTIC BLOCKMODELS: FIRST STEPS,” tech. rep., CMU, 1983.

[29] T. P. Peixoto, “Nonparametric bayesian inference of the microcanonical stochastic block model,” *Physical Review E*, vol. 95, no. 1, p. 012317, 2017.

[30] A. Rosenberg and J. Hirschberg, “V-measure: A conditional entropy-based external cluster evaluation measure,” in *Proceedings of the 2007 joint conference on empirical methods in natural language processing and computational natural language learning (EMNLP-CoNLL)*, 2007.

[31] A. Subramanian, P. Tamayo, V. K. Mootha, S. Mukherjee, B. L. Ebert, M. A. Gillette, A. Paulovich, S. L. Pomeroy, T. R. Golub, E. S. Lander, *et al.*, “Gene set enrichment analysis: a knowledge-based approach for interpreting genome-wide expression profiles,” *Proceedings of the National Academy of Sciences*, vol. 102, no. 43, pp. 15545–15550, 2005.

[32] M. V. Kuleshov, M. R. Jones, A. D. Rouillard, N. F. Fernandez, Q. Duan, Z. Wang, S. Koplev, S. L. Jenkins, K. M. Jagodnik, A. Lachmann, M. G. McDermott, C. D. Monteiro, G. W. Gundersen, and A. Ma’ayan, “Enrichr: a comprehensive gene set enrichment analysis web server 2016 update.,” *Nucleic Acids Res.*, vol. 44, no. W1, pp. W90–7, 2016.

[33] A. et al., “The Genotype-Tissue Expression (GTEx) pilot analysis: Multitissue gene regulation in humans,” *Science (80-.).*, vol. 348, pp. 648–660, may 2015.

[34] D. W. Huang, B. T. Sherman, and R. A. Lempicki, “Bioinformatics enrichment tools: paths toward the comprehensive functional analysis of large gene lists,” *Nucleic acids research*, vol. 37, no. 1, pp. 1–13, 2008.

[35] D. W. Huang, B. T. Sherman, and R. A. Lempicki, “Systematic and integrative analysis of large gene lists using david bioinformatics resources,” *Nature protocols*, vol. 4, no. 1, p. 44, 2009.

[36] T. P. Peixoto, “Efficient monte carlo and greedy heuristic for the inference of stochastic block models,” *Physical Review E*, vol. 89, no. 1, p. 012804, 2014.

[37] T. P. Peixoto, “Hierarchical block structures and high-resolution model selection in large networks,” *Phys. Rev. X*, vol. 4, no. 1, 2014.

[38] T. P. Peixoto, “Model selection and hypothesis testing for large-scale network models with overlapping groups,” *Physical Review X*, vol. 5, no. 1, p. 011033, 2015.

Acknowledgements

Ringrazio bla bla bla...

L'intero gruppo http://personalpages.to.infn.it/~caselle/BioPhys/BioPhys.html